POLITECNICO DI TORINO

Corso di Laurea Magistrale

in Automotive Engineering

Tesi di Laurea Magistrale

Insert design for sandwich composite monocoque

Relatore:
Prof. Andrea Tonoli

Candidato:
Dott. Stefano Manzi

Sommario

1. Scope

Starting from 60’s the extensive use of carbon fiber reinforced plastic (CFRP) has playing a key role in motorsport and super sport car. The main advantage of the use of CFRP structures is due to their high mechanical proprieties with the cons related to high materials and production costs.

I fully discovered the composite world during my experience in the SquadraCorse PoliTO, the FSAE team of “Politecnico di Torino”. During the years 2014-2016, I designed a carbon fiber sandwich monocoque and many aerodynamic device (i.e. front main wings, side pods etc.) with the aim of reducing weight, assure safety and looking for performance.

The lack of experience of the team in the composite world was effective, but with the help of ex-team member and many external companies across the whole design and manufacturing process, we realized a high-performance composite monocoque with higher performance in terms of specific torsional stiffness with respect of the previous 10 years.

Among all the design parameter of the monocoque, the insert dimensioning is the most critical, due to its high complexity, importance in terms of safety and weight influence in the whole frame budged; a not well-defined method for its design is present in the Squadracorse formula SAE team. For this reason, I yield this master degree thesis in the insert design.

2. Insert in composite sandwich structures

2.1. Sandwich panels introduction

A sandwich structure results from the assembly by bonding or welding of two thin skins on a lighter core that is used to keep the two skins separated, the concept idea is usually shaped by means of an I beam, see Figure 1. Facing skins are designed to bear tension/compression load meanwhile the core resists the shear loads, increases the stiffness of the structure by holding the facing skins apart; the third fundamental element of a sandwich structure is the adhesive film that joins the sandwich components and allows them to act as one unit with a high torsional and bending stiffness.

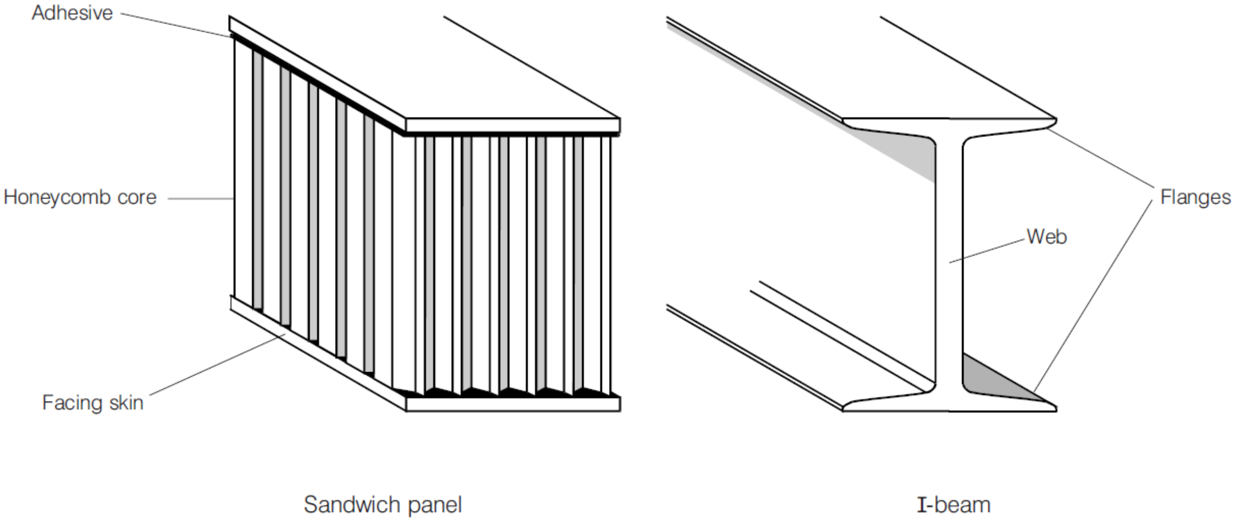

Figure 1: Construction of a sandwich panel compared to an I beam

The properties of a sandwich panels are astonishing. They have high benefits:

- light weight: separation of the outer skin is made by a very low-density material (i.e. Aluminum honeycomb 50 kg/m^3);
- high flexural rigidity**: s**eparation of the surface skins increases flexural rigidity.

Examples of sandwich panel advantage shown in Figure 2.

However, there are many cons of sandwich structure to consider:

- the risk of buckling is greater than for classical structures, both in global or local form;
- low indentation hardness/local stiffness;
- fire resistance is not good for certain core types;
- mechanical proprieties are directional (skins and core used for sandwich structures have often orthotropic characteristics), higher accuracy has to be adopted during design phase with respect to isotropic materials;
- sandwich structures are cost effective.

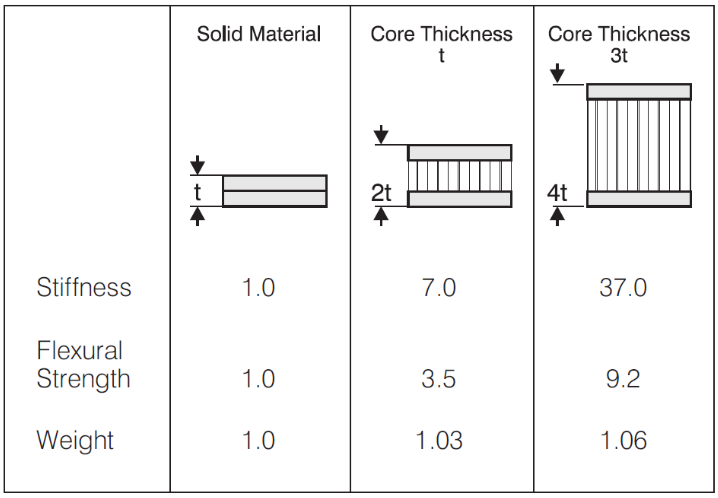

Figure 2: Stiffness and weight of sandwich panels compared to solid panels

2.2. Composite sandwich panels for racecar applications

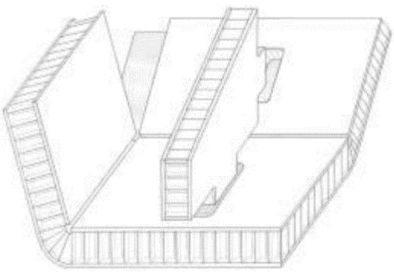

Figure 3 "cut and fold" aluminum honeycomb technique

In racing application where weight and stiffness are the main drivers, the extended use of composite materials has been used starting from 1960's by Cooper Formula 1 cars. The structure consisted of a hand worked aluminum outer skin, an aluminum honeycomb core and a GRP inner skin.

In the mid-to-late 1970's the preferred method of composite F1 chassis construction used aluminum skinned, aluminum honeycomb material fabricated using the "cut and fold" method. The tubs were formed from pre-bonded sheeting which was routed, folded and riveted/bonded using epoxy film adhesive into the appropriate shape, Figure 3.

Carbon fiber composite chassis were first introduced by the McLaren F1 team in 1980, Figure 4. They consisted of pseudo-monolithic arrangement laid up over a "male" mould or mandrel using unidirectional (UD) carbon fiber prepreg tape. The mandrel, made of cast and machined aluminum alloy, was dismantled for removal through the cockpit opening following an autoclave cure of the composite.

Figure 4: McLaren MP4/1 Carbon Monocoque

Currently, monocoque are subdivided into many sub-parts in order t to improve production process by means of "female" mould lamination. Generally, the monocoque is subdivided into an upper and a lower tubs, with the addiction of cross member section such as internal bulkheads, hoops and firewall. After the first cure, composite shells are assembled by means of modern foaming and film adhesives (Figure 5) with a post cure in autoclave.

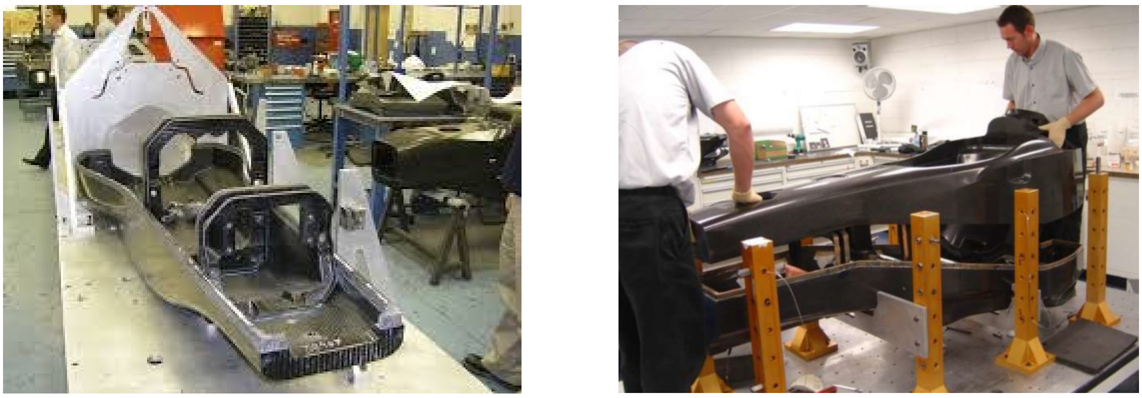

Figure 5: Modern F1 monocoque assembly

2.3. Concerns of sandwich applications and local loading effects

The unrivalled properties of sandwich constructions, particularly in bending, provide the designer with an extremely versatile, lightweight and effective configuration.

The honeycomb/composite skin construction, however, presents important but often neglected concerns regarding the effective introduction of concentrated loads from various structures attached to the chassis, in particular:

- powertrain;
- suspension;
- safety structures;
- aerodynamic devices.

In order to introduce a concentrated load (either in-plane or out-of-plane) into a honeycomb sandwich structure, the use of solid metallic/non-metallic inserts has been widely adopted. This provides a physical connection between both skins and thereby allows the load to diffuse from the point of application. The in-plane properties of the solid insert are far superior to those of the honeycomb core and therefore maintain an effective load path to the skins. In addition to the insert introduction, the ply layup configuration of the composite skins surrounding the insert is specifically designed to provide efficient load paths.

3. Insert design aspect

3.1. Inserts types

Among the whole commercially available inserts, many characterizations can be made.

3.1.1. Insert characterization according to the moment of installation

The first differentiations consist in the moment of the insert installation. Below this aspect two kind of insert types can be founded:

- hot bonded inserts;
- cold bonded inserts.

3.1.2. Insert characterization according to Potting type

Other than the timing in which the insert is fitted inside the sandwich, other variable may be described, such as potting type:

- no potting;
- partial potting: these are used where the loads to be transferred, per fixing point, are limited to in-plane and transverse forces. This is often the case where the item to be attached to the sandwich panel has a number of fixing points joined by a stiff structural part, e.g. the majority of electronic equipment; feet; A global bending moment is resolved to 'pure' forces at each fixing point; Partially potted inserts also provide mass-saving compared with fully potted inserts;
- full Potting: their static load-bearing capability is better than partially potted inserts, but inferior to through-the-thickness types;
- through the thickness: These are used when local bending moments are applied to single inserts. This enables the bending to be transferred directly to the sandwich panel face sheets. Those forces are then countered by the in-plane forces in each face sheet. Through-the-thickness inserts are also used where a bolted connection to each side of the sandwich panel is necessary.

3.1.3. <u>Insert characterization according to the insert thickness</u>

A clear overview of insert type can be found in Table 1, basically we can consider three types:

- smaller than core height;
- equal to core height;
- higher than core height.

	Moment of installation		
	Inserted before closing the face sheets, **“hot bonded”.**	Inserted in the sandwich plate, **“cold bonded”.**	
Height of insert	Smaller than or equal to core height.	Sandwich thickness.	Thicker than sandwich height, protruding.
Partial potted	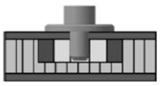	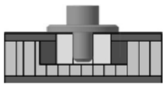	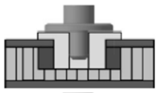
Fully potted	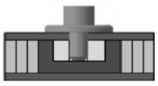	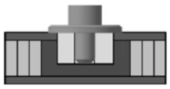	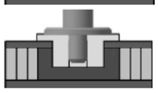
Through-the-thickness insert, clamped resp. not core connected.	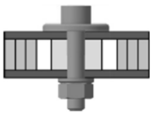	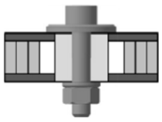	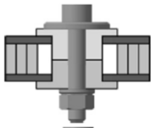
Through-the-thickness insert, core connected with potting compound.	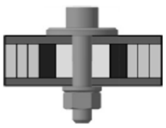	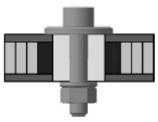	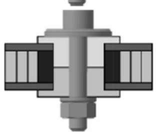

Table 1: Insert types characterization

3.2. Insert material

The majority of standard commercially-available inserts are made from certain grades of metals or combinations thereof, these being:

- Aluminum alloys**:** usually inserts are made of aluminum alloy AA 2024 (DIN AlCuMg2), solution heat treated and naturally or artificially aged, thus having the condition T85;
- CFRP: solid brick made by different layer of prepreg or SMC;
- Titanium alloys: titanium alloy TiAl6V4 (solution treated and aged) is used for applications where improved strength or special locking properties are needed.

Some remarks: if the insert is potted with an epoxy resin, there is no advantage in using a material that has a higher temperature resistance than aluminum, i.e. the resin fails at a lower temperature than the onset of damage to the insert. It is also unreasonable to select an insert material stronger than aluminum, because the strength of the system is limited by the strength of the epoxy.

3.3. Insert surface protection

Aluminium alloys

The housings made from aluminium alloy 2024 (AlCuMg2) are treated by a specified anodizing process, e.g. LN 9368, Code No. 2100 or MIL-A-8625 C.

Galvanic treatment in a sulphuric-acid bath results in a 10m to 15m thick aluminium oxide layer, which is hard and electrically nonconductive. This preserves the insert from corrosive attack and gives a suitable bonding surface. For insert systems with floating and removable nuts, the housing, plug and nut are treated in the same manner.

Titanium alloys

Titanium parts, if any, are used without any treatment because they automatically develop a protective oxide layer after machining. In order to increase protection against corrosion, an additional coating can be created using a specified anodising treatment, e.g. LN 9368, Code No. 2500.

Carbon fibre reinforced plastic

CFRP has good bonding proprieties, especially in the case of peel-ply finishing, usually no additive superficial treatment is adopted.

3.4. Embedding of the inserts – Potting materials

Commercially available insert potting materials are usually 2-part epoxy resin systems. Their inherent characteristics are usually modified by additions of micro balloons, e.g. for mass reduction; viscosity control; to aid processing (The component parts of potting compounds (resin, hardener, accelerators) are limited shelf-life materials so their usable life, storage and working conditions are controlled, e.g. workshop environment and pot-life). Other types of adhesives are sometimes used during the integration of inserts into sandwich panels, including:

- film adhesives for bonding insert flanges onto sandwich panel external surfaces, e.g. BSL 312 UL or Loctite-Hysol 9321;
- foaming adhesives for co-cured sandwich panels with inserts, e.g. Cytec/Cyanamid: FM 410-1 (150 °C); FM 37 (120 °C);

3.5. Loadings

The basic types of insert loading are summarized in Figure 6, they can be applied both in static and dynamic way. It has to be noticed that insert load introductions are notoriously weak in withstanding bending and torque loads, so they have to be avoided by constructive measures, Figure 7. Considering the remaining bidirectional force F, almost all insert sandwich configurations offer a much superior resilience against its plane parallel proportion, Fp, then against its plane normal one, Fn:

$$Fn, crit > Fp, crit$$

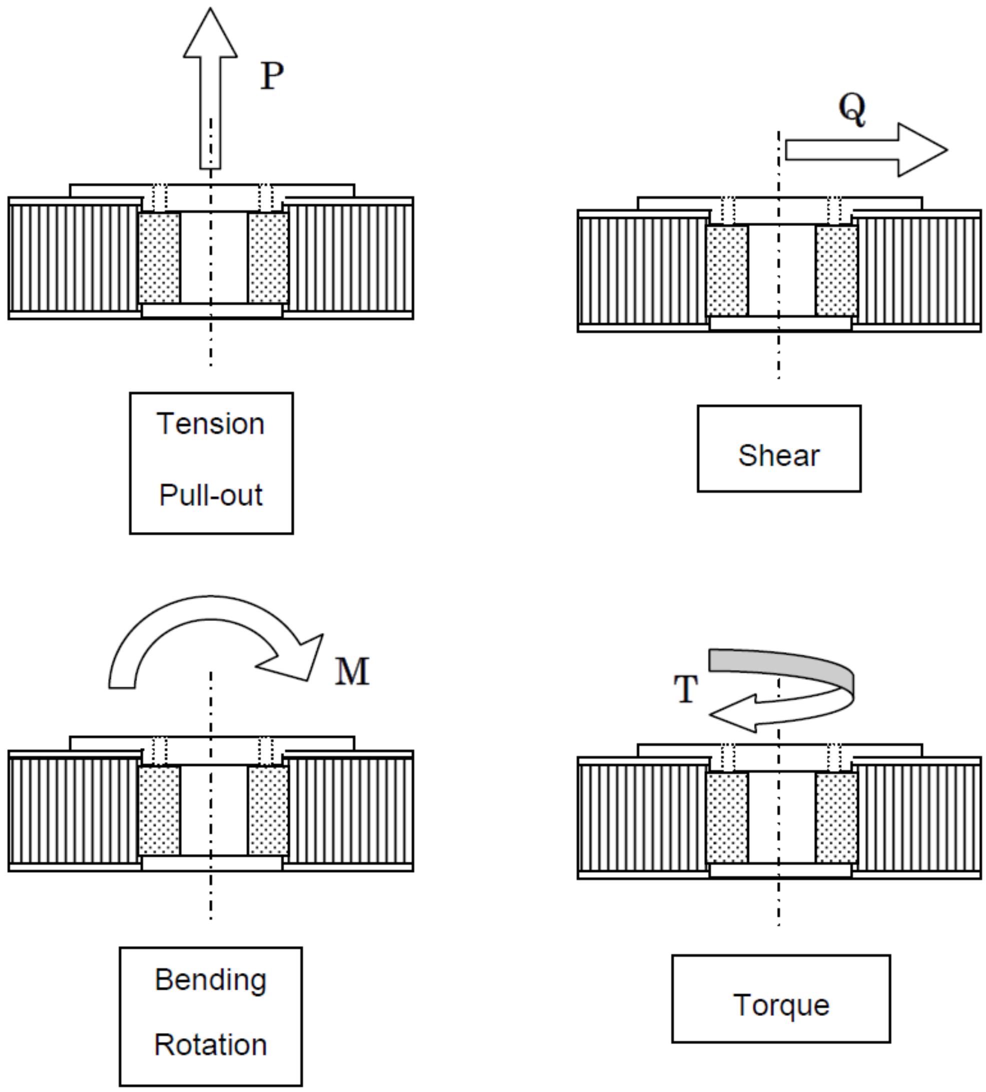

Figure 6: Insert Loadings mode

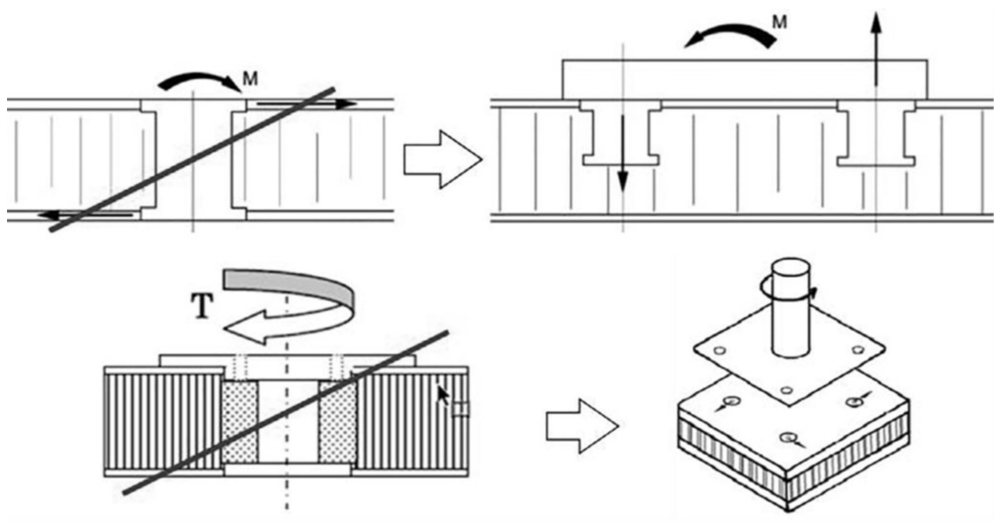

Figure 7: Constructive measures to avoid bending and torque loads on insert load introductions

It follows that the critical load for the insert designing is constituted by the critical load multiplied by a Safety Factor, that for CFRP structural part is often ≥ 2.

4. Insert dimensioning

4.1. Analytical method used in SCXV monocoque

As explained in cap 3.2, the weakest part of a CFRP sandwich panel is constituted by the composite matrix, i.e. epoxy resin; so, the insert material choice, in absence of particular requirement, it will be a trade of lightness and cheapest. Following this, the remaining degree of freedom is constituted by insert geometrical aspect and plys material thickness.

The quantity of insert present in a FSAE monocoque is huge, each dismountable vehicle component has to be provided by a mechanical connection (i.e. suspensions, main roll hoops, pedabox, HV components, seat and harness etc.), this means that each component multiplied by its n° of fixing will provide us the total number of insert to be designed.

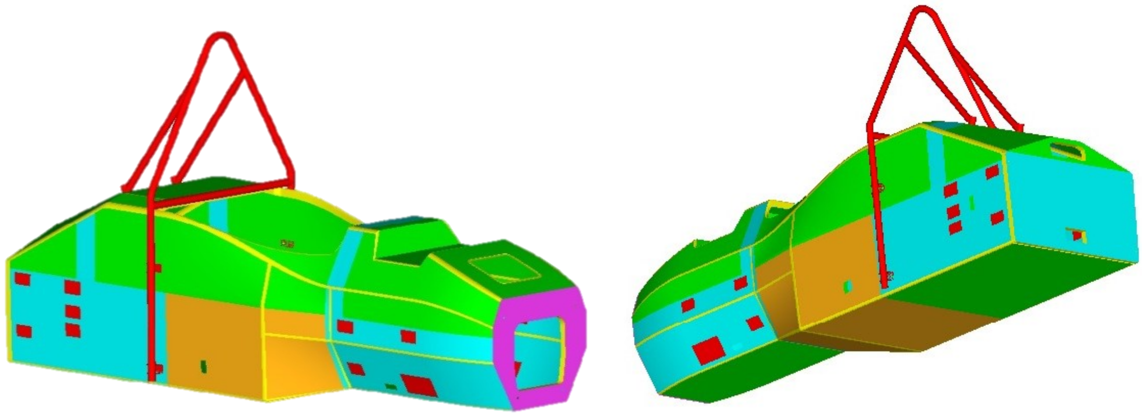

Figure 8: SCXV FEM preliminary FEM Model

In order to simplify the explanation process, the suspensions arm insert design will be presented in the following.

The suspension attachment point of a FSAE monocoque is usually constituted by a single aluminum bracket, with 2 fixing point connection (used to avoid a XY bending behavior of the mechanical fixing) to the sandwich panel and a single uniball joint for the suspension link:

Figure 9: FSAE typical suspension bracket design

The external loads coming from suspensions are mainly related to vehicle maneuvering and crash events. The insert design must be consistent with the envelope of these events.

Due to the high load case variability we selected the worst case design for a single insert with a carryover strategy in all the A arm suspension links, this choice has the pros of design simplifications and cost reduction both for the insert and the bracket assy, meanwhile the cons of overdesign in particular area i.e. rear tie rod inner link.

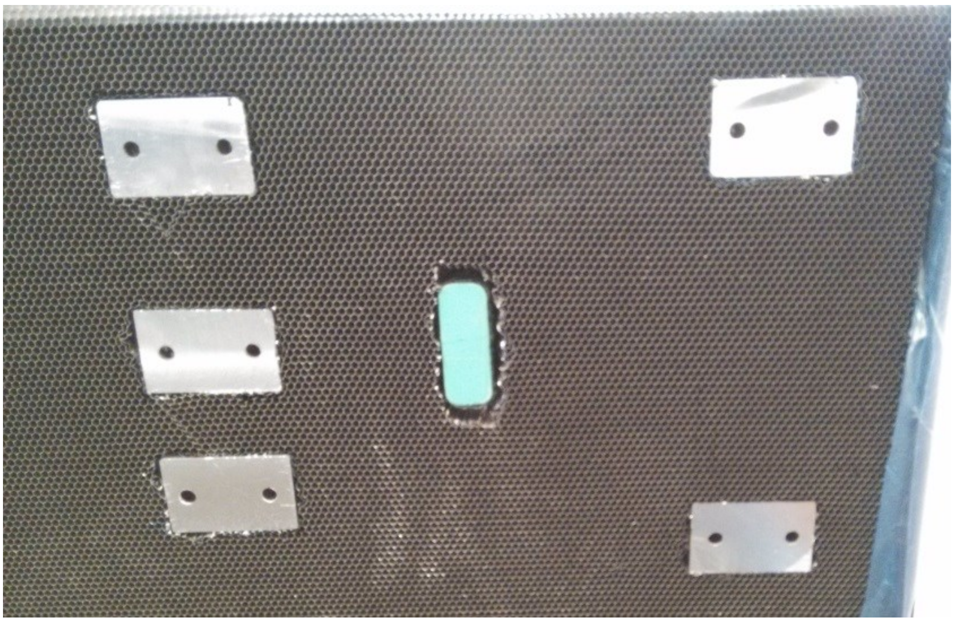

Figure 10: SCXV suspension insert positioning

For what regards vehicle dynamics load, peaks value has been taken from VI-grade maneuvering simulation (see Appendix I for the extended DATA), Braking event has been considered as suspension arm handling worst-case.

Crash loads can be estimated by suspension arms max allowable load i.e. Arms buckling condition. Suspension insert are located in critical area in a FSAE vehicle; in the event of a crash the safety of the driver and the HV system must be assured. To do so, we imposed that in any suspension attachment point the insert critical load must be higher than suspension arm critical load:

$$Finsert > Fsusp.arm$$

Suspension Arms buckling critical load has been evaluated with the Euler-Bernoulli beam theory:

F susp. Arm critical	**Load [N]**
Front UCA F	7434
Front UCA R	4366
Front LCA F	6370
Front LCA R	2730
Rear UCA F	6779
Rear UCA R	10000
Rear LCA F	5295
Rear LCA R	10000
Rear TieRod	9700
Front Rocker	5000
Rear Rocker	5000
Front Arb-Damper supp.	5000
Rear Arb-Damper supp.	5000

Once all the load cases collection is completed, we can summarize the insert design critical loads:

<table>
<tr><th>Loading type</th><th colspan="2">Load</th><th>Event</th><th>Position</th></tr>
<tr><td>Out of plane loads</td><td colspan="2">10 000 N</td><td>Crash</td><td>Rear UCA front attachment</td></tr>
<tr><td rowspan="3">In plane loads</td><td rowspan="3">1 598 N</td><td>X = 1570</td><td rowspan="3">Brake event Front</td><td rowspan="3">Front UCA front attachment</td></tr>
<tr><td>Y = -2344</td></tr>
<tr><td>Z = 297</td></tr>
</table>

As it can be seen, suspension critical loads evaluated in a direction perpendicular to the MCQ laminate are one order of magnitude higher than vehicle dynamics loads. In any case its convenient to verify out of plane loading and in plane loading since they can tell you two different indications:

- Insert perimeter: requested from out of plane loads;

$$P = \frac{F}{T \cdot \sigma_{\perp}}$$

- Insert area: requested from out of plane loads;

$$A = \frac{F}{\sigma_{=}}$$

Material data required for these evaluations are ply perimeter shear strength and ply in shear strength. Usually it’s possible to obtain this information from pre-preg datasheet provided by the material supplier or, as we made in Squadracorse, get it from material characterization test (see ASTM D3039 or equivalent ISO).

Prepreg ply material: Deltapreg prepreg M46J Toray balanced with resin DT120:

Denomination	**GG200T(M46J) -DT120-42**
Test Conditions	Room Temp.
TENSILE TEST	
Tensile strength (MPa)	680
Tensile modulus (GPa)	95

COMPRESSION TEST	
Compression strength (MPa)	440
Compression modulus (GPa)	80
IN-PLAIN SHEAR	
Shear strength (MPa)	80
Shear modulus (GPa)	3
OUT-OF-PLAIN SHEAR	
Shear strength (MPa)	80
INSERT-PLY INTERFACE BONDING	
Shear strength (MPa)	10

The monocoque General material layup has been evaluated from vehicle Global Loads:

- torsional stiffness;
- front crash;
- side crash;
- rollover;
- accumulator system protection.

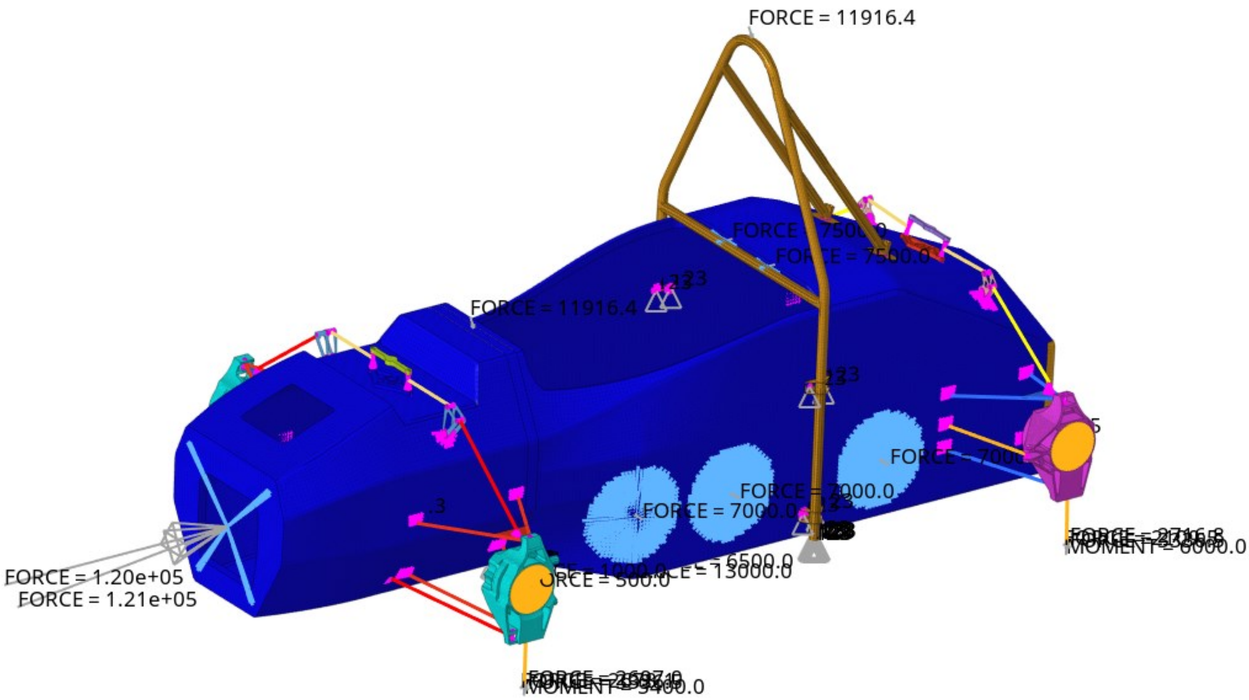

Figure 11: SCXV full vehicle model for general lay-up design

Local reinforcements are instead the result of local loads coming from:

- pedal box;
- suspension arms;
- steering rack;
- driver harnesses;
- HV Components attachments (battery pack, inverters, DCDCs. Etc.

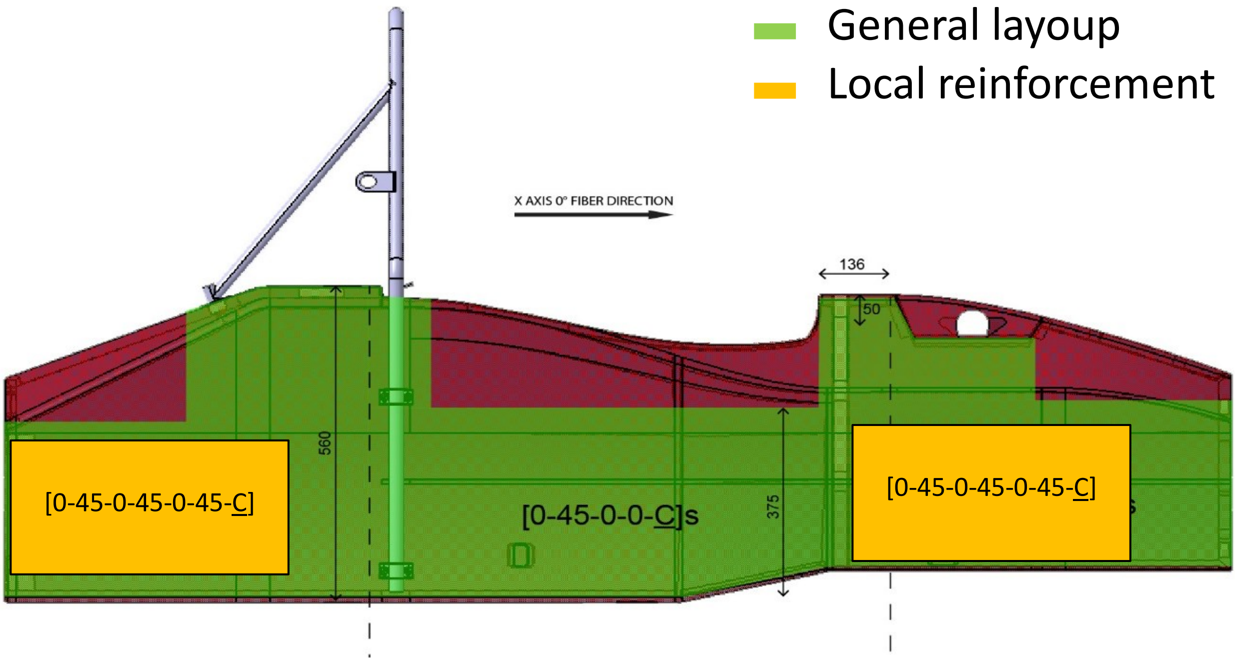

Figure 12: SCXV side Layup

From **out of plane loads** (F=10000N) and out-of-plain ply max shear $\sigma_{\perp}$ =80MPa, P will be a linear function of the sandwich ply thickness, that for CFRP sandwich is ≥ 1mm. With the hypothesis of a balanced sandwich [0-45-0-45-0-45-C] in suspensions area, ply thickness is equal to 1.32mm -> P=95mm.

From **in-plane loads** (F=1598 N) and DT120 resin shear strength ($\sigma_{\perp}$ =10MPa) it is possible to design the insert minimum bonding area -> A= 160mm^2.

Here below the drawing of the suspension bracket insert:

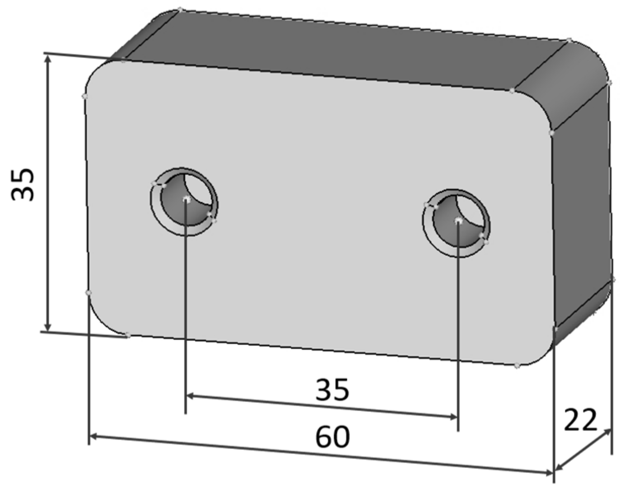

Figure 13: Suspension insert dimensions

Insert dimension check can easily be summarized as:

Load case	Value	Requested	Status	Margin
Out of plane loads	Perimeter [mm]	95	190	2
In-plane loads	Area [mm^2]	160	2100	13

As expected in-plane load cases are less stringent with respect to out of plane one, and insert minimum dimension has been validated.

The procedure descripted so far can give you only a rough indication of insert minimum dimension and imply many simplifications. First of all, the procedure considers only a single ply against the external loads, instead of the sandwich panel:

- outer ply for in plane loads;
- inner ply for out of plane loads.

Doing so the, contribution of the remaining Inner/outer ply is totally neglected. Secondary, core contribution is not considered, that means that also max allowed shear stress of the core (Aluminum honeycomb or foam usually) is not evaluated; in the case of potting material, we are not aware of possible detach between the insert and the core material. The difference between insert without/with core connection is descripted in the next table:

Insert Type	**Figure**
Through-the-thickness insert, clamped resp. not core connected. -> insert type used in SCXV monocoque	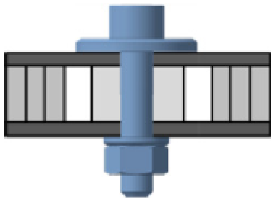
Through-the-thickness insert, core connected with potting compound.	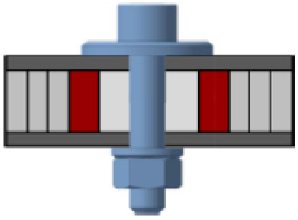

The two types of connection generate a very different stress trend on the sandwich panel.

The procedure descripted in CAP 4.3, case of out of plane loads, can be correctly addressed only for backing plates design.

Another issue of previous descripted design consists in the same dimensions between Suspension bracket and suspension insert. In this case there is a strong transition between insert load out of plane load and sandwich load:

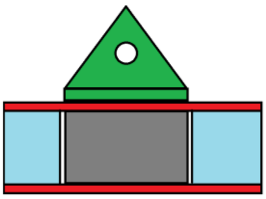

Figure 14: SCXV Bracket and MCQ assy

More in general its suggested to get sandwich connections, such as washer, backplates or bracket higher than the potting diameter. Example:

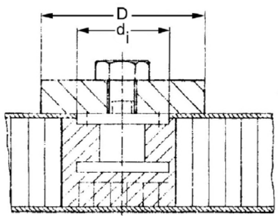

Figure 15: Example of proper overlap between Insert radius and backplate

4.2. Analytical Modelling: ECSS Anti-plane extension theory

The European Cooperation for Space Standardisation (ECSS) is an organisation that is involved in space sector engineering standardization. In 2011 this organization made a pubblications regards insert dimensioning. In the following I've extracted the main steps that suit for my purpose of CFRP inserts designing. Full details can be founded in the original text: "Insert design handbook" ECSS Secretariat, ESA-ESTEC.

Differently for what considered in the SC design, and in particular for potting insert design, loads are transmitted to different load-bearing components, i.e.:

- in-plane loads are transmitted to face sheets;
- transverse loads are transmitted to the honeycomb core.

This can be considered, with good approximation, a useful boost for pre-design calculation.

The use of classical anti-plane sandwich theories is fine for predicting global load response characteristics, the weak point of this theorem is a rough approximation of the complicated load-transfer in proximity to the load application points. An accurate modelling of load response that takes into account also local effects like core transverse flexibility can be provided by finite element modelling or by the high-order sandwich theory. Both of them are very costly solution, the first scenario requires a Computer aided design with FEM method meanwhile the latter cannot be solved in a closed form and requires a numerical approach. An exception to the problem is present in the case of sandwich plates with inserts subjected to compressive or tensile out-of-plane loads. In this case the fracture mechanism is most of the time a shear rupture of the honeycomb in the potting-core interface. The peak core stress is correctly estimated by the classical antiplane theory so, for these particular cases, it's possible to obtain similar result in terms of shear stress distribution with respect to high order theory.

The mode takes into account a cylindrical symmetry with two main variables:

- Z: sandwich thickness coordinate;
- R: radial distance from load application position.

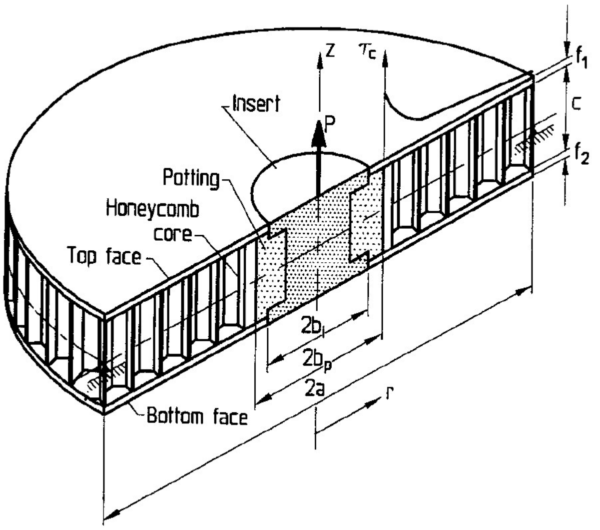

Figure 16: ECSS Anti-plane theory cylindrical coordinate system

The first hypothesis is constituted by an infinitely rigid insert body with radius *bi*, meanwhile potting compound from *bi < r < bp* and honeycomb *r > bp* can be deformable in shear. The needs of deformable potting are required for the prediction of the correct shear field in the potting-honeycomb interface.

For fully potted inserts the failure occurs by shear rupture of the core surrounding the potting, especially by shear rupture of the undoubled core foils, indicated in the following image as *WT planes*.

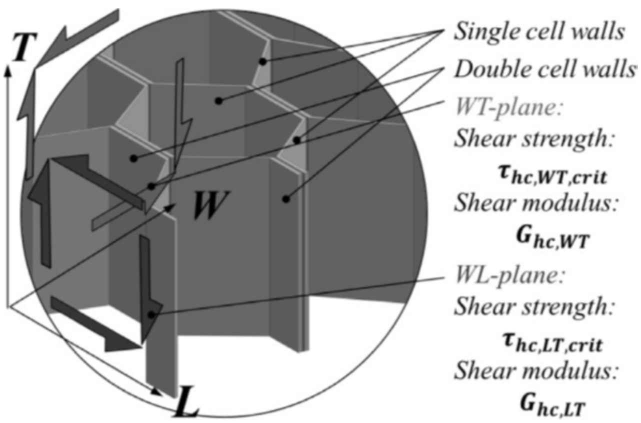

Figure 17: Effects of W and L direction in the honeycomb morphology

Therefore, the limiting capability property is the core shear strength Tau*c crit* and the insert capability *Pcrit* increases quasi-linearly by increasing the core height *c*.

The sandwich panel maintains the equilibrium with the external load P with a radial transverse shear stress resultant Qr(r). In this particular case Qr(r) can be evaluated as:

$$Q_r(\mathrm{r}) = \frac{\mathrm{P}}{2\pi r}, r \geq b_i$$

By plotting our particular case where P=10kN and b_p=17, the transverse shear stress has a hyperbolic trend:

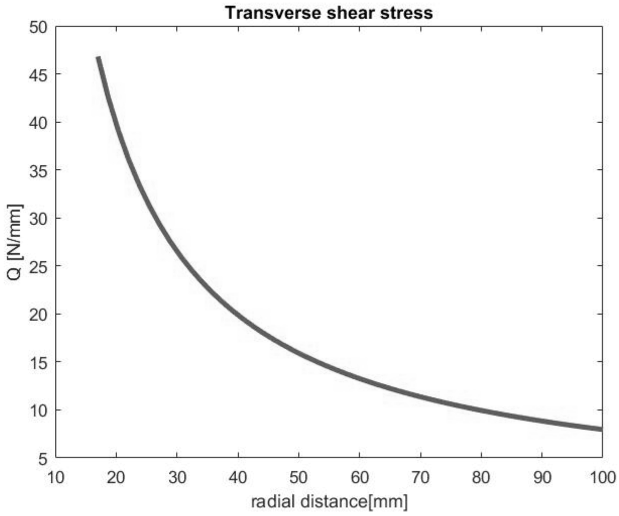

The second assumption of the anti-plane theory comes from the high diversity between core and face sheets elastic moduli, i.e.:

$$E_c \ll E_{f1}, E_{f2}$$

The in-plane stiffness of the core can be totally neglected $E_c \approx 0$, and the core shear stress is nearly constant over the core thickness. These approximations can highly simplify core shear stress and face sheets calculation:

$$\tau_c(r) = \frac{Q_r(r)}{D}\frac{E_{f1}f_1E_{f2}f_2d}{\left(E_{f1}f_1 + E_{f2}f_2\right)} = \frac{\boldsymbol{P}}{2\pi rD}\frac{E_{f1}f_1E_{f2}f_2d}{\left(E_{f1}f_1 + E_{f2}f_2\right)}$$

$$\tau_{f1}(r,z)=\frac{Q_r(r)}{D}\frac{E_{f1}}{2}\left[\left((d-e)+\frac{f_1}{2}\right)^2-z^2\right]=\frac{P}{2\pi r D}\frac{E_{f1}}{2}\left[\left((d-e)+\frac{f_1}{2}\right)^2-z^2\right]$$

Valid from: $(d-e)-\frac{f_1}{2}\le z\le(d-e)+\frac{f_1}{2}$

$$\tau_{f2}(r,z)=\frac{Q_r(r)}{D}\frac{E_{f2}}{2}\left[\left(e+\frac{f_2}{2}\right)^2-z^2\right]=\frac{P}{2\pi r D}\frac{E_{f2}}{2}\left[\left(e+\frac{f_2}{2}\right)^2-z^2\right]$$

Valid from: $-e-\frac{f_2}{2}\le z\le -e+\frac{f_2}{2}$

Where:

$\tau_c(r)$ = core (potting compound and honeycomb core) shear stress.

$\tau_{f1}(r,z)$ = shear stress in top face sheet.

$\tau_{f2}(r,z)$ = shear stress in bottom face sheet.

z = thickness coordinate measured from the 'neutral surface' of the core.

c = core thickness.

d = $d=f_1/2+c+f_2/2$; distance between the face sheet middle surfaces.

e $e\approx E_{f1}f_1d/(E_{f1}f_1+E_{f2}f_2)$; distance from 'neutral surface' of the core to the middle surface of the bottom face sheet.

f_1 = thicknesses of top face sheet.

f_2 = thicknesses of bottom face sheet.

E_{f1} = elastic moduli of top face sheet.

E_{f2} = elastic moduli of bottom face sheet.

For $E_c \ll E_{f1}, E_{f2}$ the equation for the sandwich plate stiffness is given by:

$$D\approx\frac{E_{f1}f_{f1}^3}{12(1-\nu_{f1}^2)}+\frac{E_{f2}f_{f2}^3}{12(1-\nu_{f2}^2)}+\frac{E_{f1}f_1E_{f2}f_2d^2}{E_{f1}f_1+E_{f2}f_2}$$

ν_{f1}, ν_{f2} = Poisson's ratios of the face sheet materials.

Third assumption of the model by considering $c \gg f1, f2$ give us the possibility to neglect the first two terms of equation of D.

The final expression for core and face sheet shear stress are:

$$\tau_c(r) = \frac{Q_r(r)}{D} \quad = \frac{\boldsymbol{P}}{2\pi r D}$$

$$\tau_{f1}(r,z) = \frac{\boldsymbol{P}}{2\pi r D}\frac{1}{f_1}\left[\left((d-e)+\frac{f_1}{2}\right)-z\right]$$

Valid from: $(d-e)-\frac{f_1}{2} \leq z \leq (d-e)+\frac{f_1}{2}$

$$\tau_{f2}(r,z) = \frac{\boldsymbol{P}}{2\pi r D}\frac{1}{f_2}\left[\left(e+\frac{f_2}{2}\right)+z\right]$$

Valid from: $-e-\frac{f_2}{2} \leq z \leq -e+\frac{f_2}{2}$

Applying the previous equations to our particular case the following Plots can be obtained:

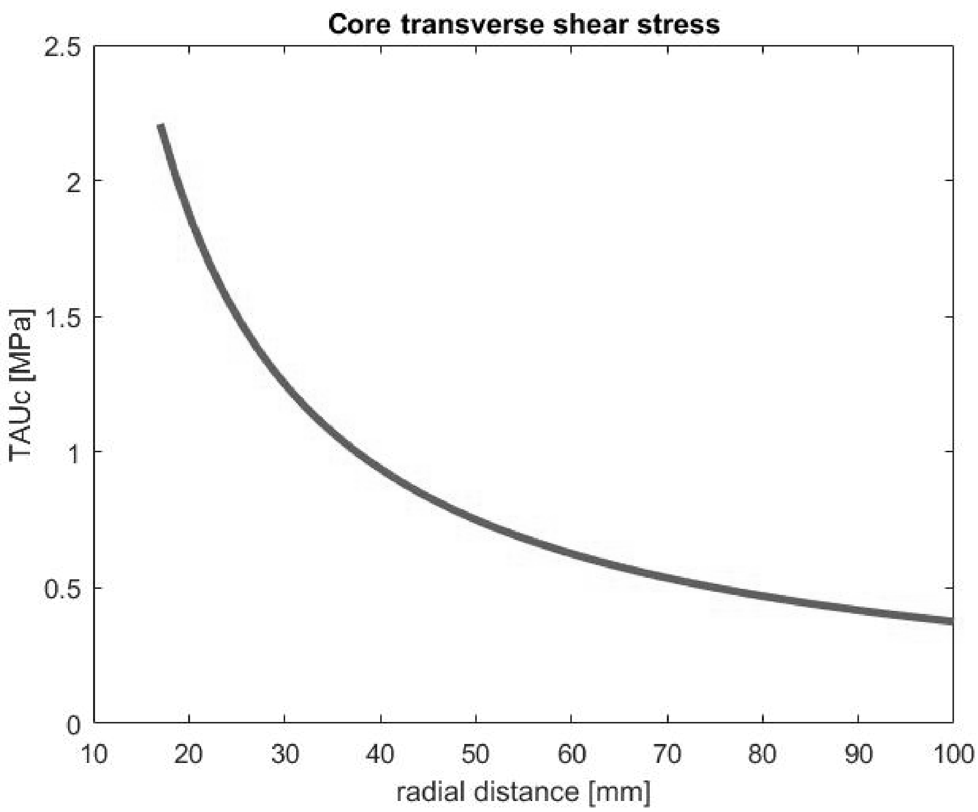

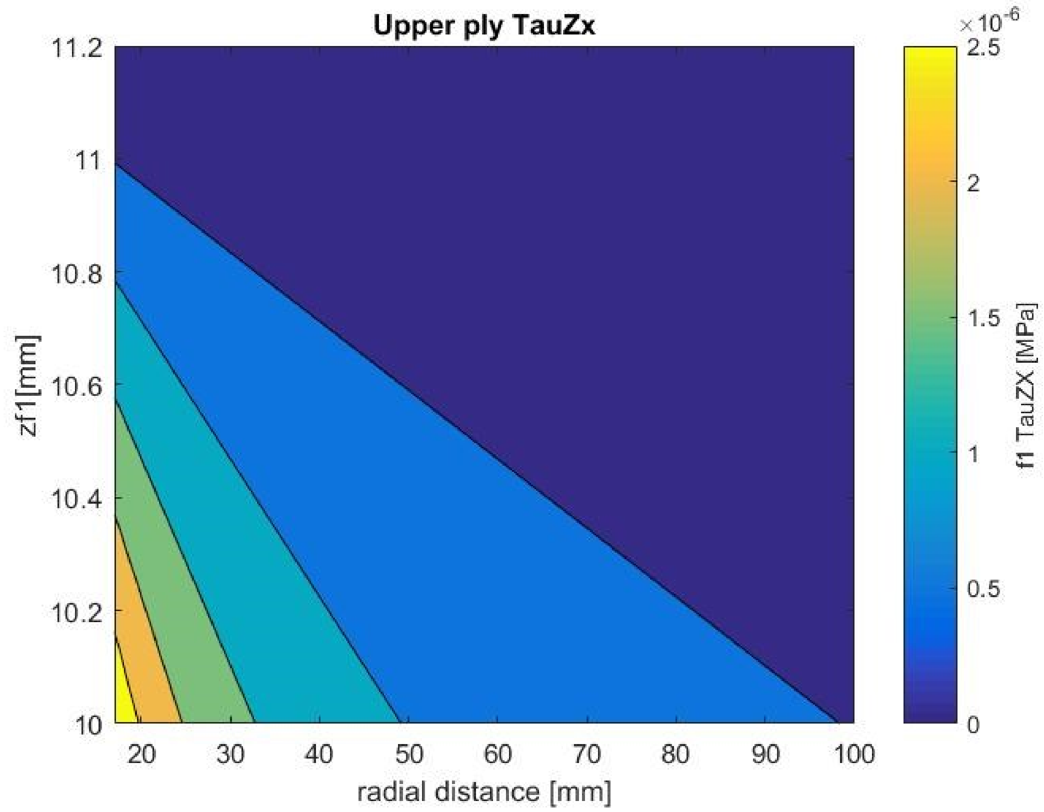

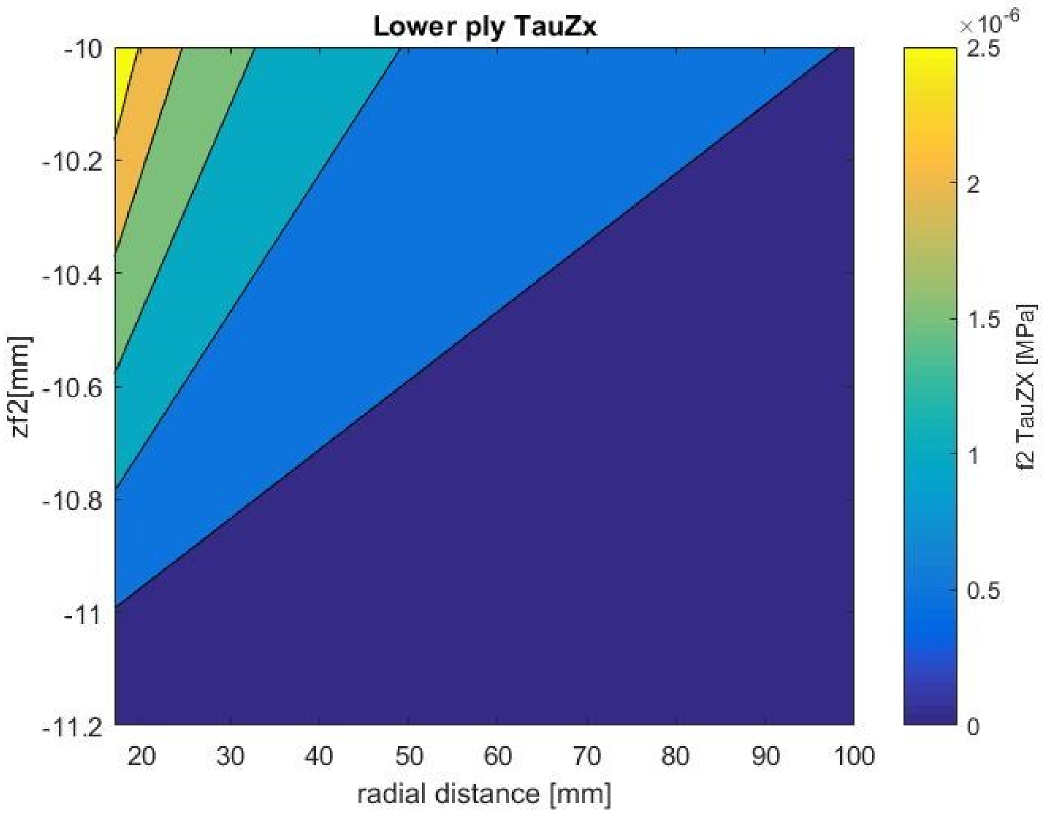

As seen in the radial transverse shear stress resultant Qr(r), also the core, f1 and f2 plys have a hyperbolic shear stress trend. The value of the shear stress over the thickness c is constant, meanwhile shear stress increases linearly over the ply thickness by approaching the core interface. As discussed, in the case of fully Potted inserts the failure occurs typically next to the potting to honeycomb interface at $r=b_p$ even though the shear stress field in the potting compound is higher. This is explained by higher potting compound strength than the honeycomb. At r=bp, the core reaches the maximum core allowable shear stress $\tau_{c,max}$. With the aid of the previous equation we get:

$$\tau_{c\max} = \tau_c(r = b_p) = \frac{\boldsymbol{P}}{2\pi b_p d} = \frac{\boldsymbol{P}}{2\pi b_p d}$$

By knowing the actual core shear strength of the core, we can finally estimate the static load capability of the designed insert:

$$\boldsymbol{P}_{crit} = 2\pi b_p d\, \tau_{ccrit}$$

The obtained value is valid both for tensile and compressive load case of single insert.

In the case of multiple inserts, like the example of suspension attachment point bracket, there is an interaction between different insert loaded together. Generally, the interaction is influenced by the insert proximity distance and load case type.

First of all, it's possible to understand if we deal with proximity problem by the equation:

$$a \le 5(b_{p1} + b_{p2})$$

Where:

- b_{p1}: potting radius of insert 1;
- b_{p2}: potting radius of insert 2;
- a: insert centre-to-centre distance.

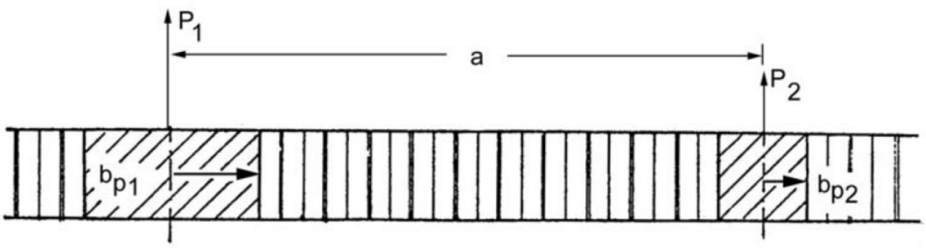

Figure 18: Insert proximity evaluation scheme

If the previous equation is satisfied, we deal we proximity insert interference, in this case the insert capability is reduced by the coefficient η_{IS1}, by the equation:

$$P^{*}_{SS} = P_{SS}\eta_{IC}$$

Then we have a differentiation in load reduction upon the loading condition, in the case of:

- Insert loaded in the same direction (i.e. both in compressive out of plane loading), we consider:

$$\eta_{IS1} = \frac{b_{p1}/b_{p2}}{1+b_{p1}/b_{p2}}\left(1+\frac{a}{5b_{p1}}\frac{1}{1+b_{p1}/b_{p2}}\right)$$

  Taking into account SC bracket layout η_{IS1} reduces the insert capability up to 58%.

- Insert loaded in the opposite direction:

$$\eta_{IC} = 0.9 \quad \text{for} \quad a \leq 5(b_{p1} + b_{p2})$$

If the equation is not satisfied there is no interaction between inserts and their load capability will be not reduced:

$$\eta_{IS1} = \eta_{IS2} = 1 \quad \text{for } a > 5(b_{p1} + b_{p2})$$

4.3. Insert dimensioning with a FEM Model

A dedicated FEM model has been produced in the Hyperworks environment, and compared with the result given by the Anti-plane theory described in CAP 4.

The realization of the 3D fem model is based on several 3D Brick solid elements for the core material, potting compound and insert modelling, the use of 2D shell elements has been instead applied for sandwich CFRP skins. The use of a solid core is useful to provide accurate prediction for local response of the honeycomb in the areas where local bending phenomena cannot be ignored.

It has to be noted however, that the use of a 3D modelling for the core material in composite manufact design is not commonly spread due to its exponential increment of modelling effort. Similar results can be founded with 2d modelling when local effects are not the focus of the FEM analysis, i.e. whole vehicle modelling.

4.3.1. FEM model geometry

The 3d model for the insert FEM analysis is constituted by a sandwich panel of dimensions 600*400mm, the insert is located in the middle of it in order to avoid boundary effects from FEM Boundary conditions. All the node of the elements present in the FEM geometry are linked in an equivalent node form.

Th insert is embedded in the sandwich structure via the potting compounds. Reference quotes can be founded below, it has been taked from the insert supplier Shur-Lok choosing a through the thickness insert with M6 connection and potting holes.

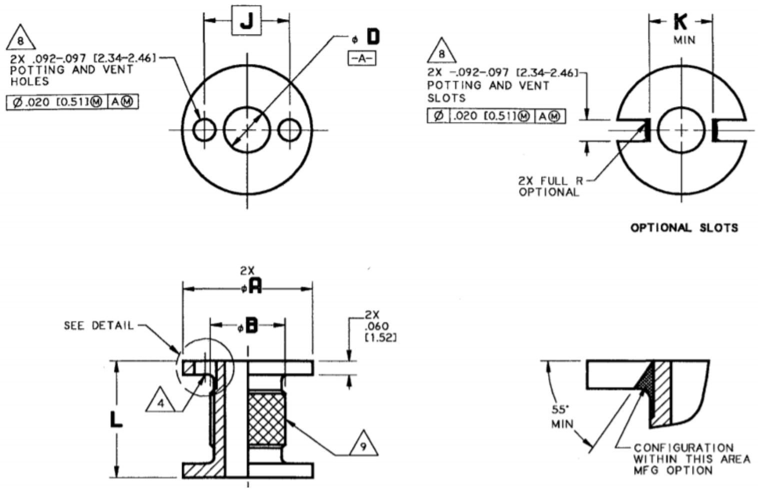

SIZE CODE	ϕA +.000 −.010 [0.00] [0.25]	ϕB	ϕD CLEARANCE HOLE	J BASIC	K MIN	L MIN (5)	INSTALLATION HOLE SIZE
4	.685 [17.40]	.37 [9.4]	.256–.263 [6.50–6.68]	.467 [11.86]	.360 [9.14]	.312 [7.92]	.686–.691 [17.42–17.55]
M6			.243–.249 [6.17–6.32]				

The potting radius has been evaluated with the analytical model (anti-plane model, CAP 4) and it's equal to 34mm.

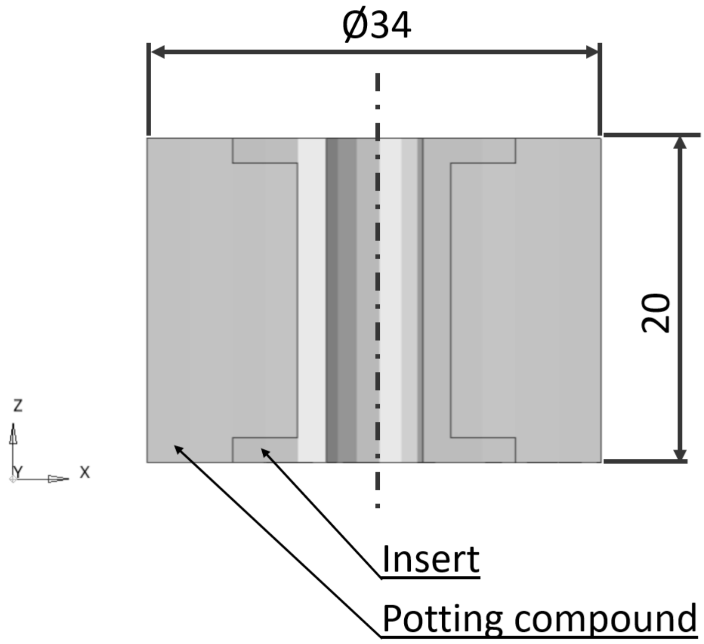

4.3.2. FEM model element description

The pre-process phase starts from the Finite element creation.

A sandwich panel is usually modelled with only 2d membrane elements, but in this case, where there is a focus in the insert-potting and potting-core interfaces also, solid elements has been used.

2D elements are the best design for CFRP plys modelling, a bias approach has been used, so a minimum dimension of 2mm has been used for elements nearby the application point. The elements dimension grows up to 10mm nearby sandwich panel edges.

4.3.3. FEM model material cards

The properties applied to the 2d and 3d elements are of type:

- PBEAM for bolts 1D elements:

Name	Value
Solver Keyword	PBEAM
Name	screw
ID	5
Color	
Include	[Master Model]
Defined	☑
Card Image	PBEAM
Material	(4) steel
User Comments	Hide In Menu/Export
Beam Section	(1) circle_section.1
PBEAM_CARD3 =	0
Aa	28.274333882308
I1a	63.617251235193
I2a	63.617251235193
I12a	0
Ja	127.23450247039
NSMa	
CONTINUATION LINE 2	☐
CONTINUATION LINE 5	☐
⊞ CONTINUATION LINE 6	☑
PBEAMX	☐

- PCOMP for cfrp plys 2D elements;

Name	Value
Solver Keyword	MAT8
Name	M46J
ID	2
Color	
Include	[Master Model]
Defined	☑
Card Image	MAT8
User Comments	Do Not Export
E1	95000.0
E2	95000.0
NU12	
G12	3000.0
G1Z	
G2Z	
RHO	1.63e-09
A1	
A2	
TREF	
Xt	680.0
Xc	440.0
Yt	680.0
Yc	440.0
S	70.0

- PSOLID for Core, Inserts and Potting 3D elements. It follows the Material cards used in the FEM model for the PSOLID elements:

Name	Value
Solver Keyword	MAT9ORT
Name	Honeycomb
ID	1
Color	
Include	[Master Model]
Defined	☑
Card Image	MAT9ORT
User Comments	Hide In Menu/Export
E1	1.0
E2	1.0
E3	1310.0
NU12	
NU23	
NU31	
RHO	8.33e-11
G12	81.0
G23	400.0
G31	576.0
A1	
A2	
A3	
TREF	
GE	
MATX...	☐

Name	Value
Solver Keyword	MAT1
Name	Alluminum
ID	3
Color	
Include	[Master Model]
Defined	☑
Card Image	MAT1
User Comments	Hide In Menu/Export
E	68900.0
G	
NU	0.33
RHO	2.7e-09

Name	Value
Solver Keyword	MAT1
Name	Potting
ID	5
Color	
Include	[Master Model]
Defined	☑
Card Image	MAT1
User Comments	Hide In Menu/Export
E	2300.0
G	900.0
NU	
RHO	1.25e-09
A	
TREF	
GE	
ST	38.0
SC	48.0
SS	34.5

Honeycomb material value from supplier datasheets:

5052 Alloy Hexagonal Aluminum Honeycomb – Specification Grade

Both CR-PAA and CR III corrosion-resistant coating

Hexcel Honeycomb Designation Cell Size – Alloy – Foil Gauge	Nominal Density pcf	Compressive					Crush Strength psi	Plate Shear					
		Bare		Stabilized				L Direction			W Direction		
		Strength psi		Strength psi		Modulus ksi		Strength psi		Modulus ksi	Strength psi		Modulus ksi
		typ	min	typ	min	typ	typ	typ	min	typ	typ	min	typ
1/4 – 5052 – .0025	5.2	690	500	760	510	190	335	410	360	82.0	265	200	35.4

As can be seen from the Hexcel honeycomb datasheet, and as usually occurs, only the shear modulus in the W and L direction are provides, the core shear modulus in the 12 direction i.e. G_C is not provided. From measurements made by ECSS, the shear modulus is a function of the loading and decrease as a result of the core non-linear behavior i.e. shear buckling of single foils at half of expected value. It's common to consider the core shear module (G12) equal to:

$$G_c = {G_W}/{3}$$

Where:

G_W shear modulus in W-direction.

Potting material value from supplier datasheets:

Dexter Hysol	EA 9309 NA		Paste
Epoxy - two part			
Test Methods: ASTM		March 92	
Physical		**Mechanical**	
Colour	Grey	τ (RT)	34.5 MPa
Viscosity	A=8, B=0.04 Pa.s	τ (82°C)	4.1 MPa
S.G.	1.1	τ (wet)	-
Shelf life	1 yr./RT	Peel (-)	6.83 Nmm^{-1}
Pot/Work life	40 min.	σ_t	37.9 MPa
Tg	56°C (54°C wet)	σ_c	48.3 MPa
$T_{Service}$	71°C	E	2070 MPa
CTE (°C)	-	G	900 MPa
Thermal cond.	-	Elongation	10 %
Resistivity: Vol.	-	Tear strength	-
Surf.	-	H (Shore D)	80

Notes: Tensile lap shear strength and Service temperature - ASTM D 1002. Tensile properties - ASTM D 638. Compressive - ASTM D 638. Peel - ASTM D 1876. Electrical ASTM D 149/150: Dielectric constant @1kHz RT: 4.29. Dissipation factor @1kHz RT: 0.016.

4.3.4. FEM model boundary conditions

The boundary conditions of the FEM model are similar to the Analytical model described in CAP 4. Two load cases have been considered for the analysis:

- load case 1: crash events equal to the suspension arm buckling load;
- load case 2: maximum handling forces from braking maneuver.

The constraint of the sandwich panel represents a simply supported condition only in **the lower ply**, applied on the whole sandwich perimeter in isostatic condition. The idea is to consider the sample panel as an extract of the Formula SAE side chassis, ad depicted:

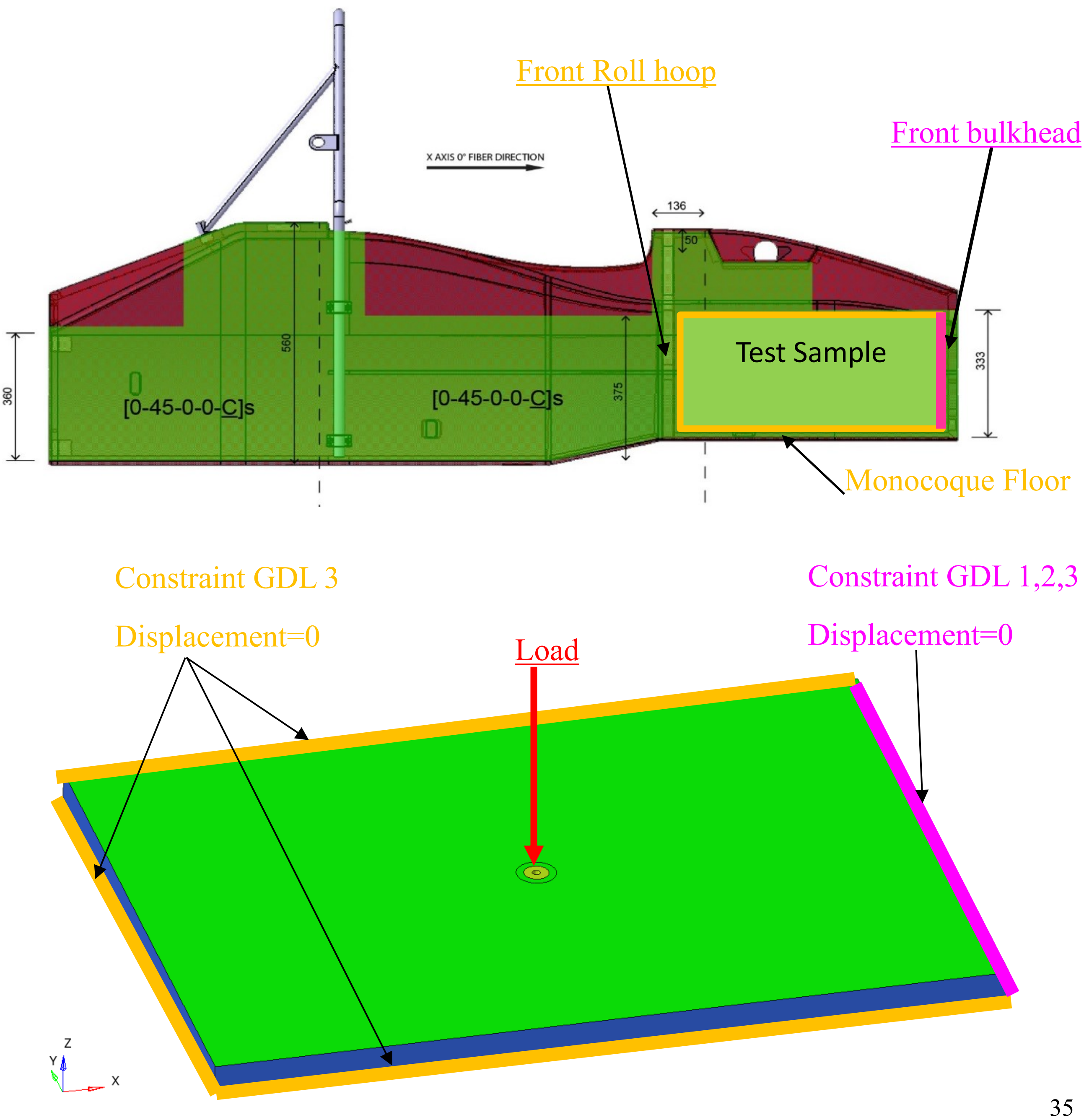

4.3.5. FEM model post processing

The post processing of a FEM model is the key part of the whole FEM analysis. From the result is possible to derive prediction of the model behaviour and understand if the modelling has been done correctly.

First of all, the Post processing of the critical load case, the crash event will be presented:

Displacement field:

- overall Z displacement of the sandwich panel top view:

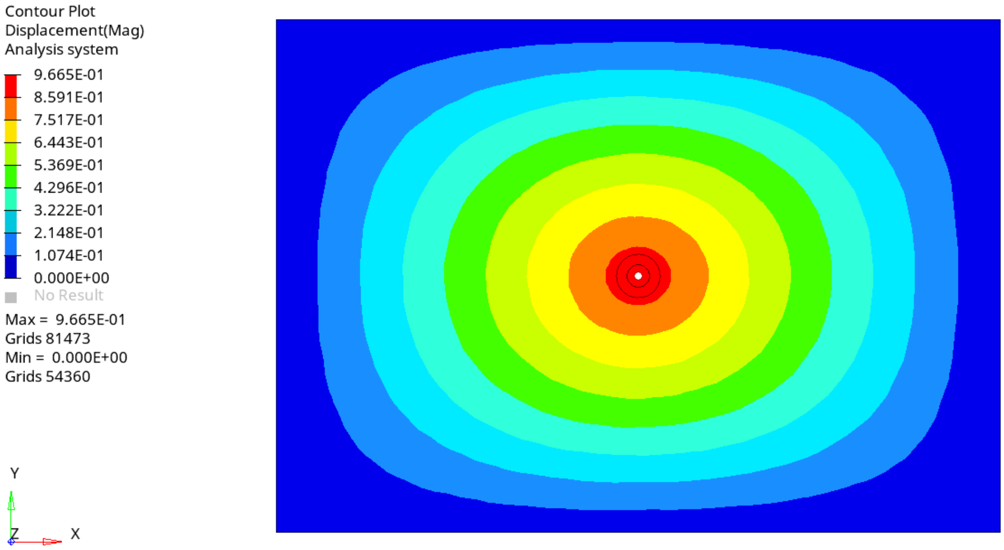

- overall Z displacement of the sandwich panel cross section at Y=0, render multiplier x20:

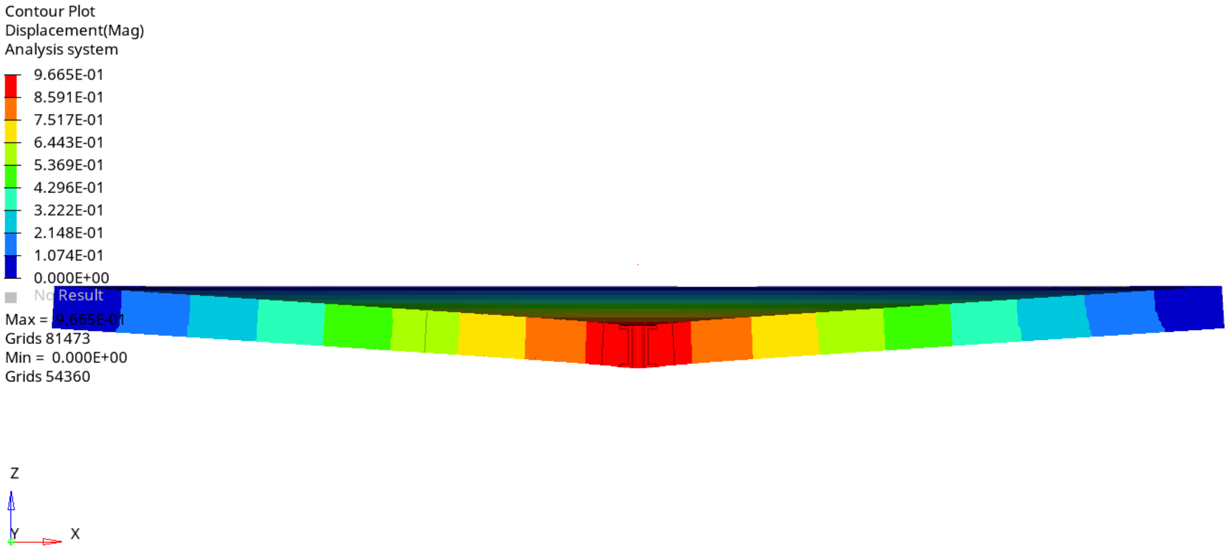

Honeycomb plots:

- honeycomb $\sigma_{ZZ,core}$: tensile/compressive stress

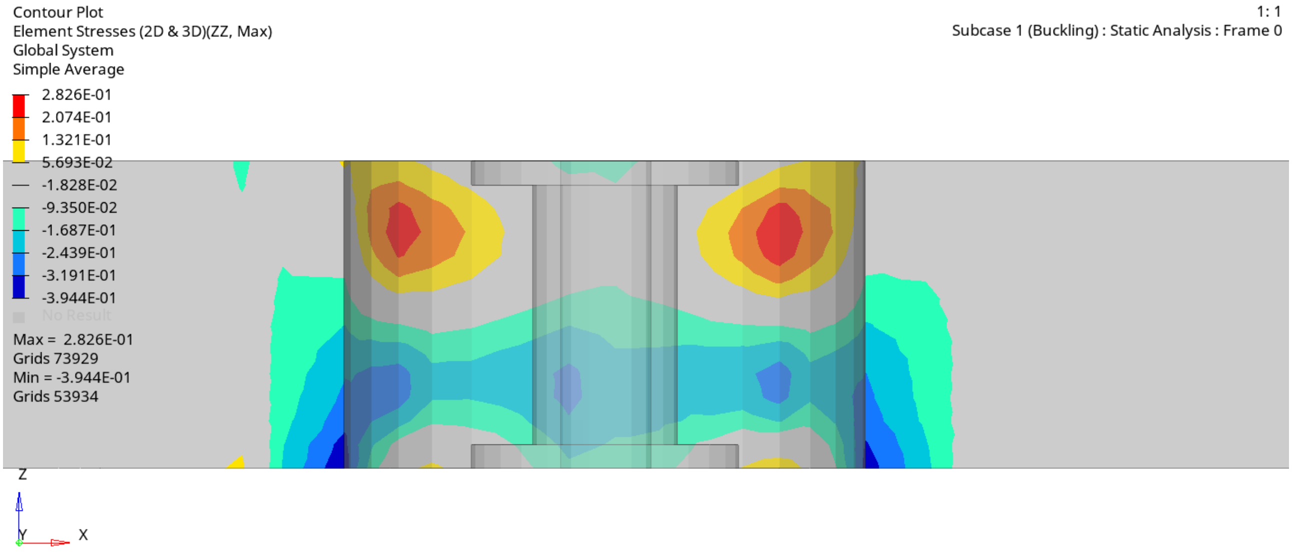

- honeycomb $\tau_{ZX,core}$: transverse core shear stress

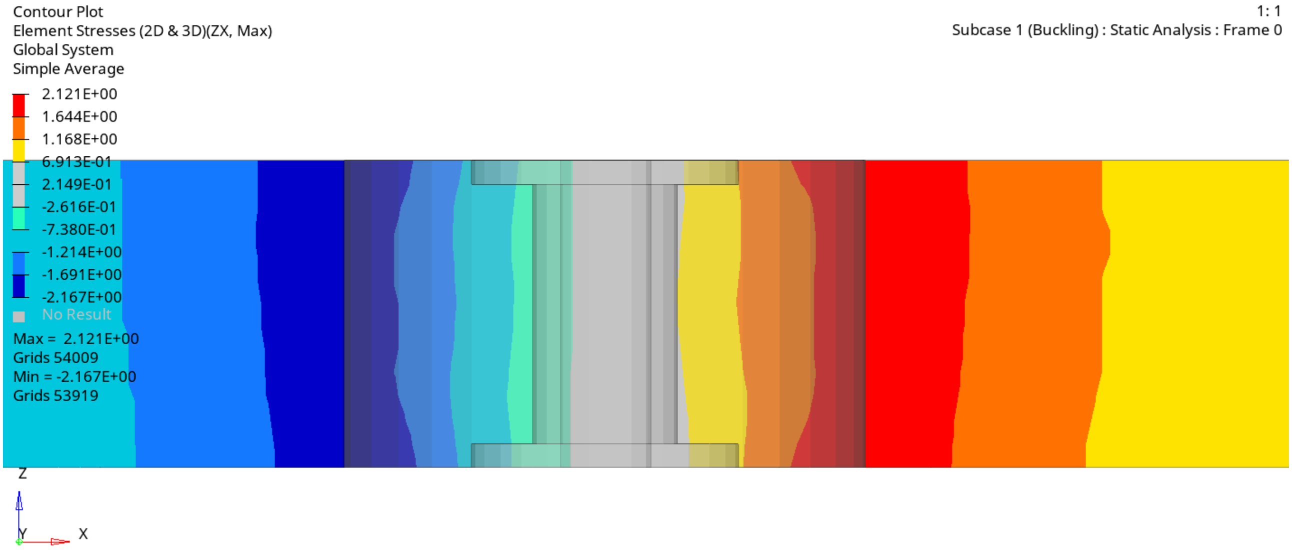

Potting Plots:

- potting $\sigma_{ZZ,core}$: tensile/compressive stress

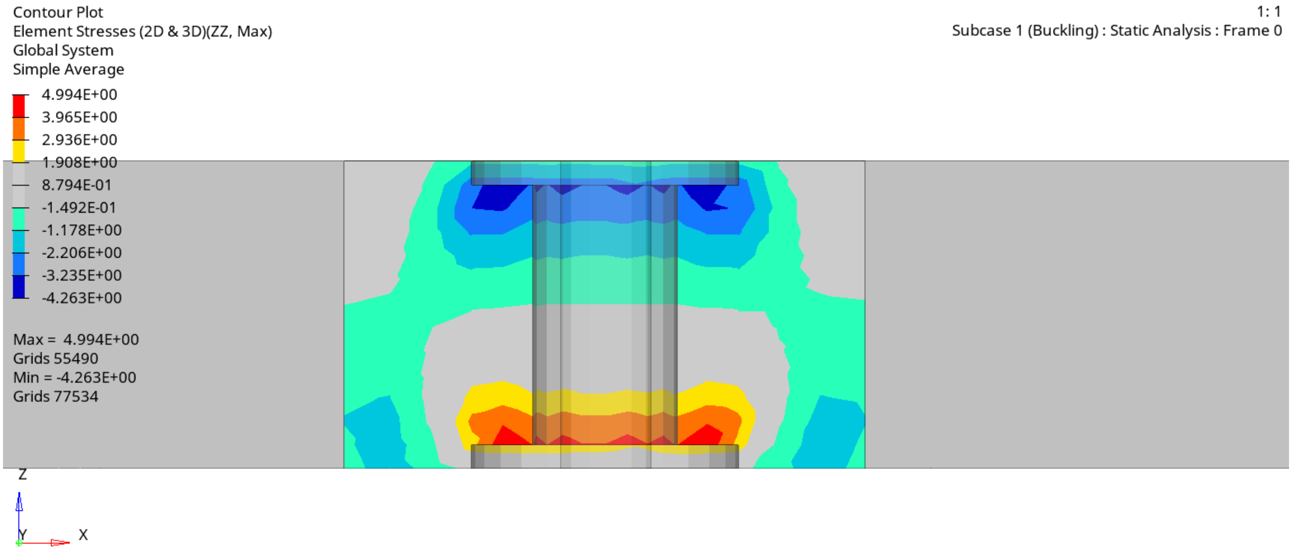

- potting $\tau_{ZX,core}$: transverse core shear stress

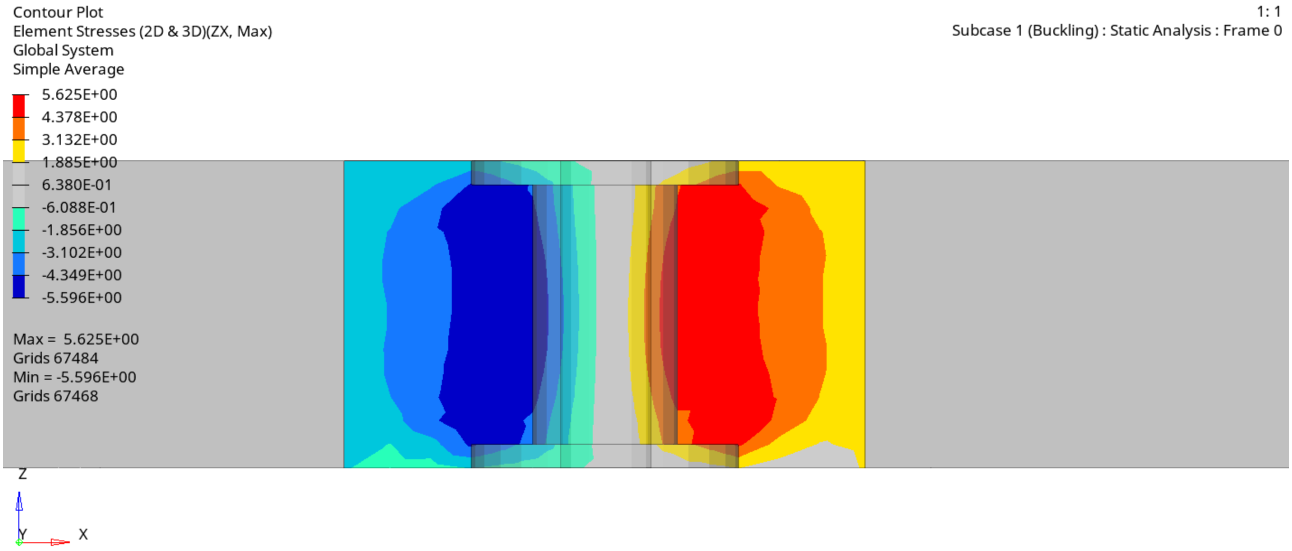

CFRP upper ply Plots:

The ply post processing usually is made by using a Failure Criteria, that in this case follows the Tsai-Wu formulation. One denotes the Tsai-Wu the number a such that:

- If a < 1: no ply rupture occurs;
- If a > 1: rupture occurs in the ply considered.

- Ply1 composite failure according to Tsai-Wu criteria:

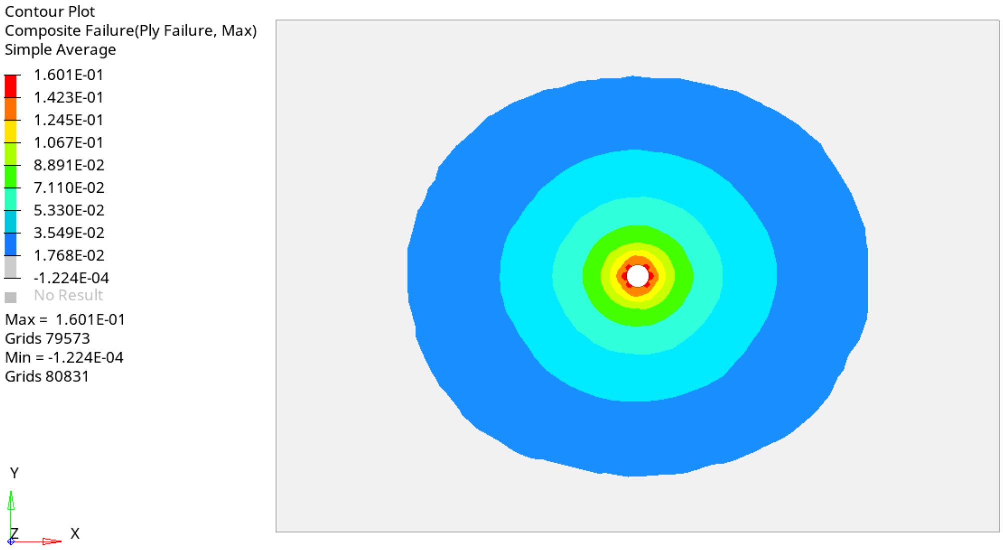

- Ply1 bond failure according to Tsai-Wu criteria:

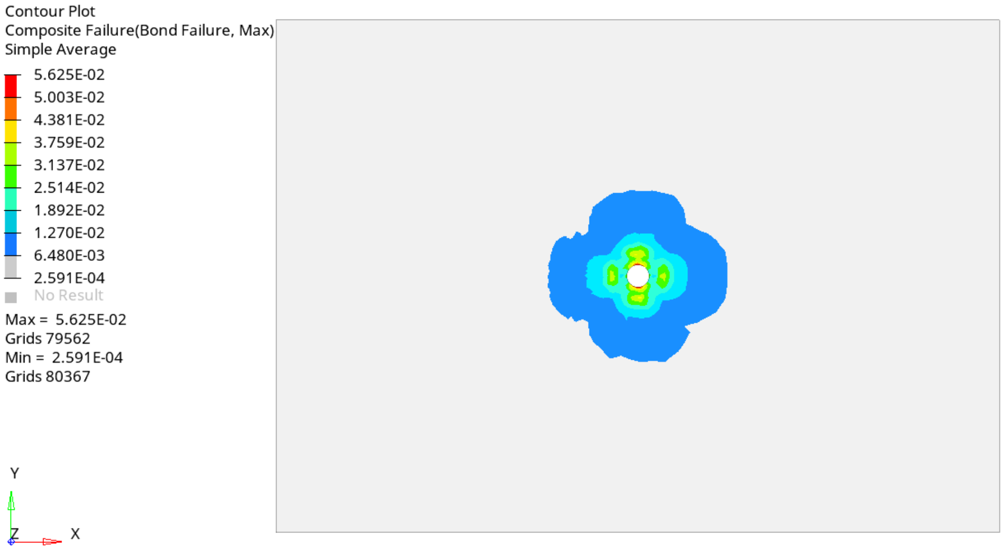

CFRP lower ply Plots:

- Ply 2 composite failure according to Tsai-Wu criteria:

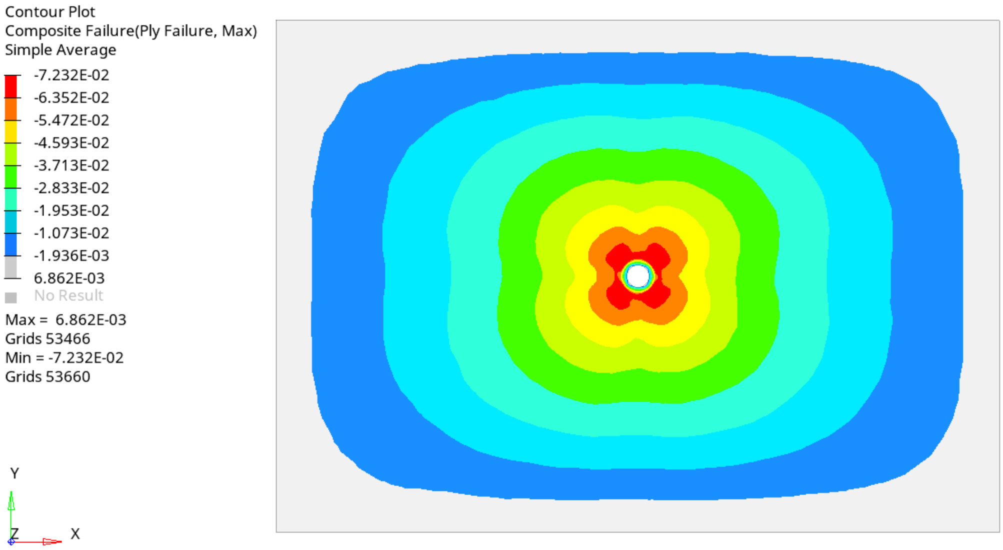

- Ply 2 bond failure according to Tsai-Wu criteria:

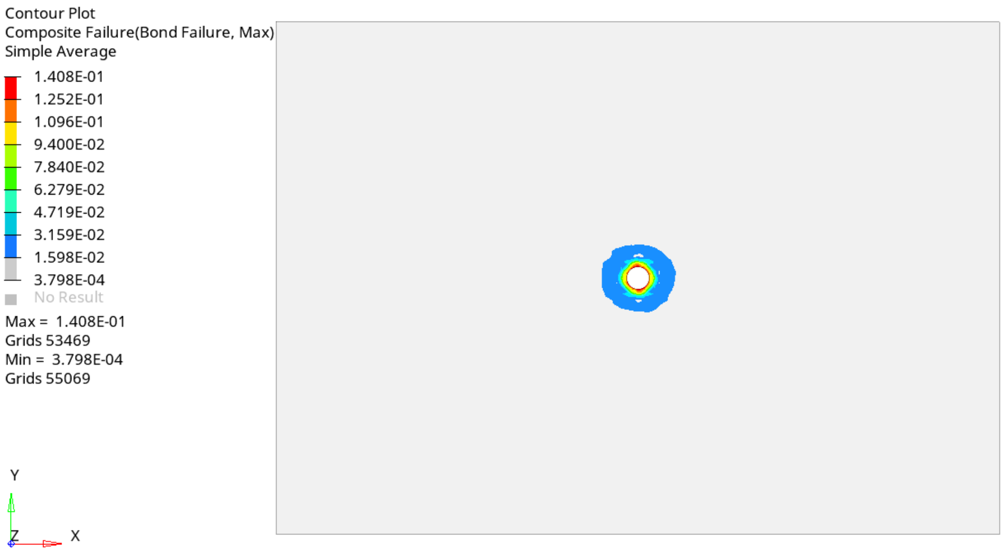

4.4. Dimensioning procedure comparison

The adoption of a dedicated FEM model can provide additional information with respect to the Analytical Model. In fact, with the analytical model we verify only the core shear stress in the core material while being not aware of Insert, Potting, and ply tensile status.

With the Anti-plane theory, we made 4 hypotheses:

- aluminium inserts body totally undeformable;
- constant shear stress over the core thickness;
- hyperbolic Core shear stress trend;
- failure in the potting-core interface;

Let's verify the **first** hypothesis follow the plot of the Von Mises Strain of the Insert Assy in a Y=0 section, it's clearly visible that the insert is dark blue, according to the legenda, its body is almost undeformed compared to the model elements.

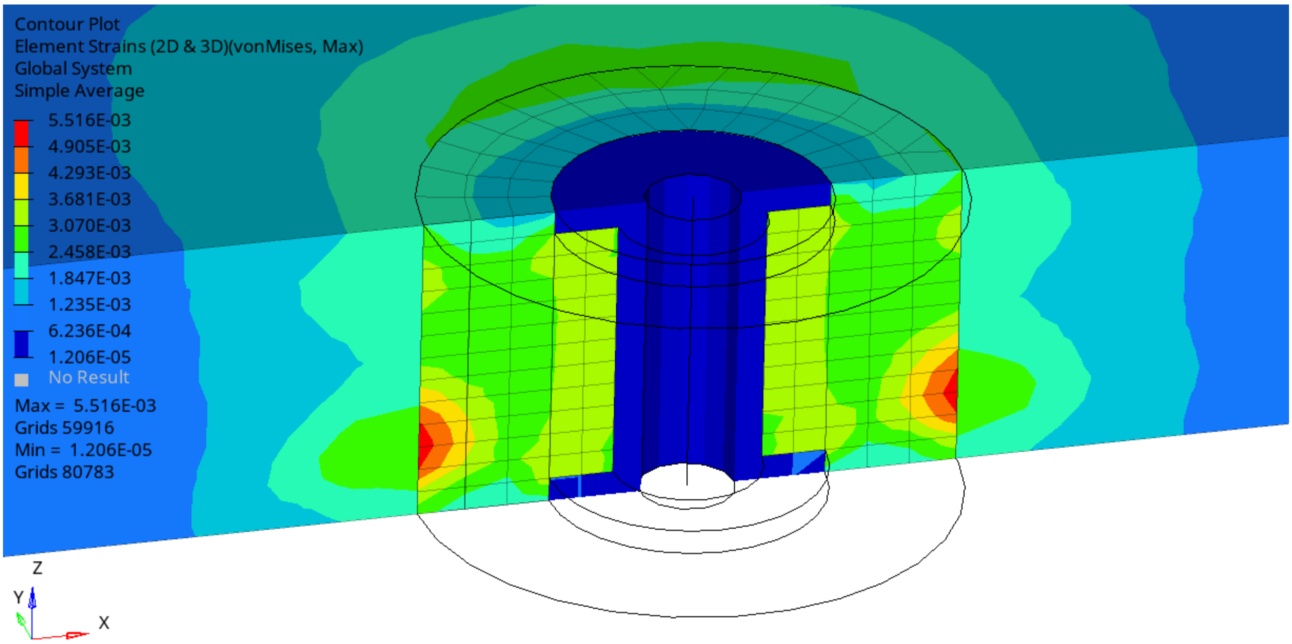

Second hypothesis, the plot shows the Shear stress of the honeycomb material along its thickness and distance from the insert axis. The stress is constant over the core thickness.

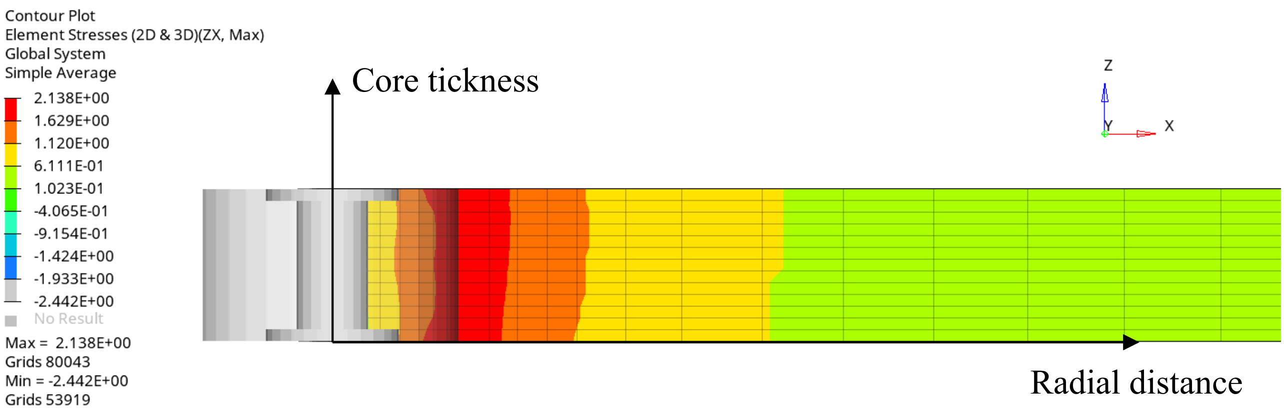

Third hypothesis, Hyperbolic trend of the honeycomb shear stress in the radial direction (for the FEM model this corresponds to the 31 direction of the core material). In this case it's possible to make a 1:1 comparison between Analytical and Finite Element Method results. The Fem result is a good representation within ad error of less than 5%.

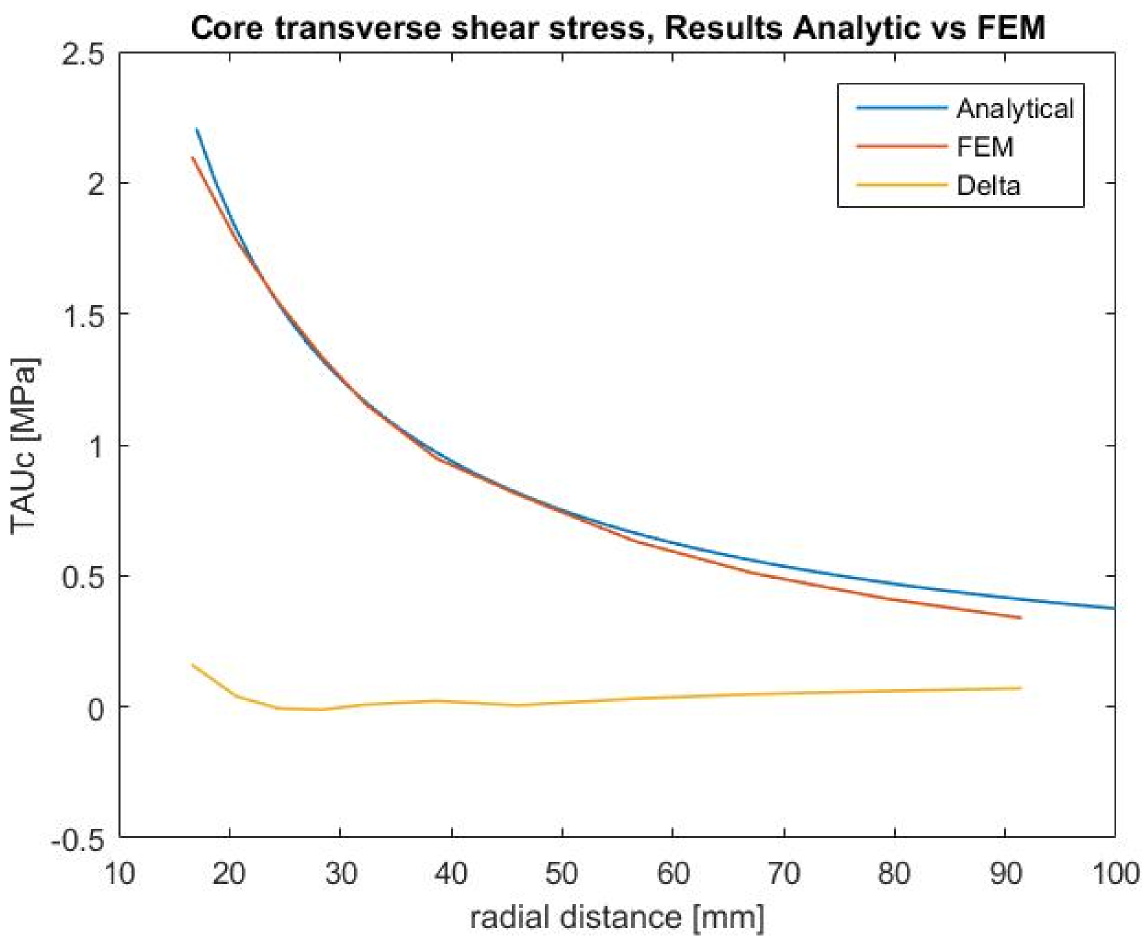

Fourth hypotesis, the failure point. The FEM model used for the simulation is a Linear Elastic and its not possible to simulate the failure of the insert assembly, but its possible to understand the model behavior and find the weak point by comparing the Elements status with respect to the material limits. By checking the margin value of the core materiale in the TAU field the following table it's in line with the last hypotesis:

DATA / Topic		FEM Model – Through the thickness with potting		
		[MPa]	Reference value [MPa]	Margin
Core	Sigma ZZ	0.3	5.2	17.3
		-0.4	-5.2	13.0
	TAU ZX	2.1	3.2	1.5
	TAU ZY	1.9	2.7	1.4
Potting	Sigma ZZ	5.0	38.0	7.6
		-4.3	-48.0	11.2
	TAU ZX	5.6	34.5	6.2
		-5.6	-34.5	6.2

DATA / Topic		FEM Model – Through the thickness insert with potting		
		Tsai-Wu Failure criteria	Reference Value	Margin
Ply 1	Ply Failure	0.2	<1	6.3
	Bond Failure	0.1	<1	16.7
Ply 2	Ply Failure	0.1	<1	14.3
	Bond Failure	0.1	<1	7.1

All of the 4 hypotesis of the Anti-plane model are correctly represented in the FEM mode, this means that the model is reliable and can be used for further consideration.

5. Suspension insert FEM dimensioning

In this chapter the FEM methodology will be applied to the specific case of the Suspension bracket attachment points. The specimen used for the 3D modelling is constituted by a panel of dimensions 600*400mm, simply supported, subjected to a compressive out-of-plane load. The loading is representing the suspension arm buckling with a total force of 10kN.

By following the previous BCs, three solution will be compared with a linear elastic model:

- **Baseline model:** a single through the thickness insert block not core connected.
- **Case study 1:** a single through the thickness insert block core connected via potting compound;
- **Case study 2:** two through the thickness insert block not core connected via potting compound.

5.1. Baseline model– Squadracorse insert

The 3d geometry of the baseline model is in line to what depicted in CAP 4.1. Material data according to CAP 4.3.3 and constraint iso 4.3.4. An overview of the Baseline model follows:

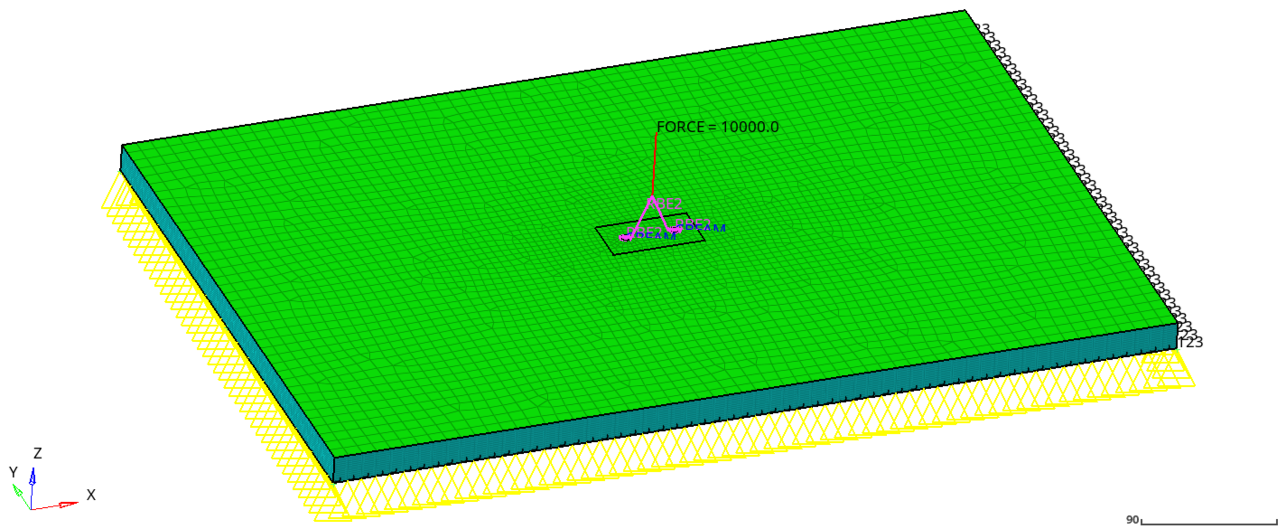

Baseline model - Displacement field:

- overall Z displacement of the sandwich panel Top view:

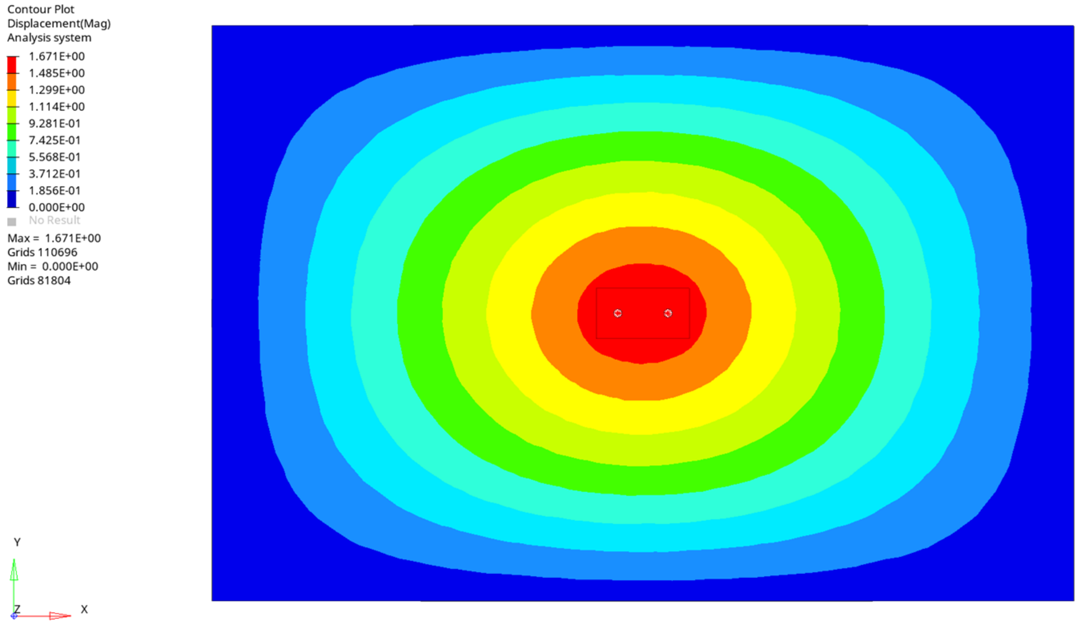

- overall Z displacement of the sandwich panel cross section at Y=0, render multiplier x20:

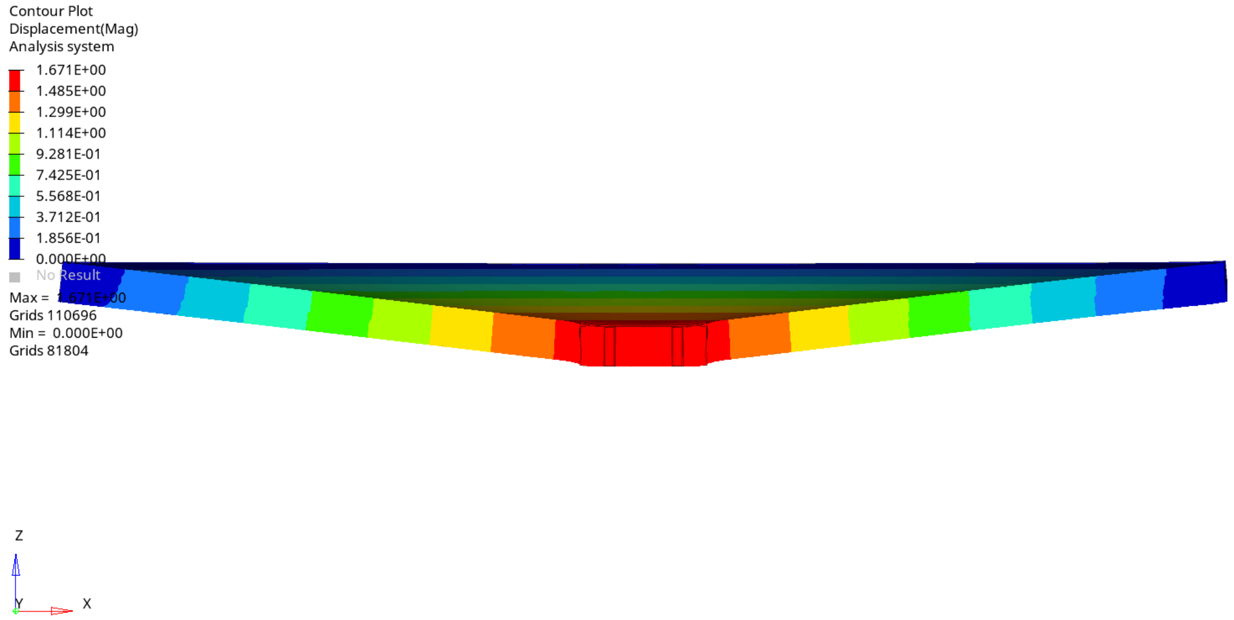

Baseline model - Honeycomb plots:

- honeycomb $\sigma_{ZZ,core}$: tensile/compressive stress

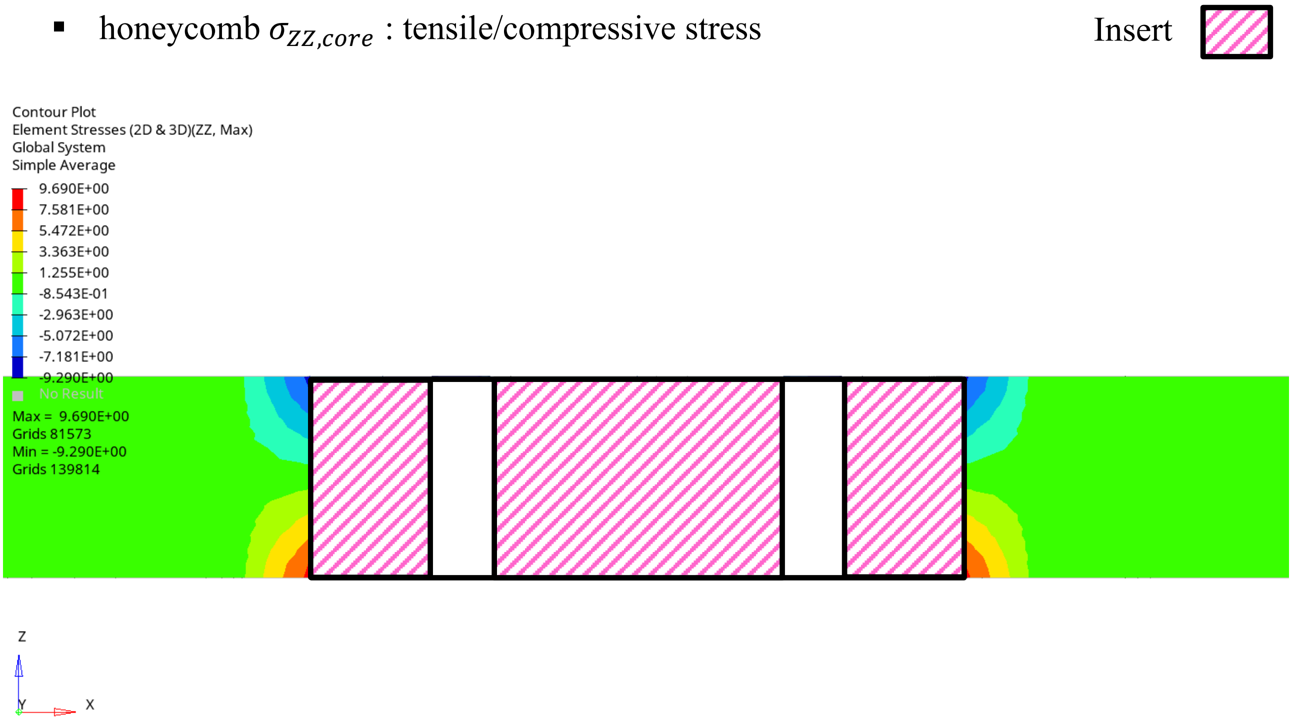

- honeycomb $\tau_{ZX,core}$: transverse core shear stress

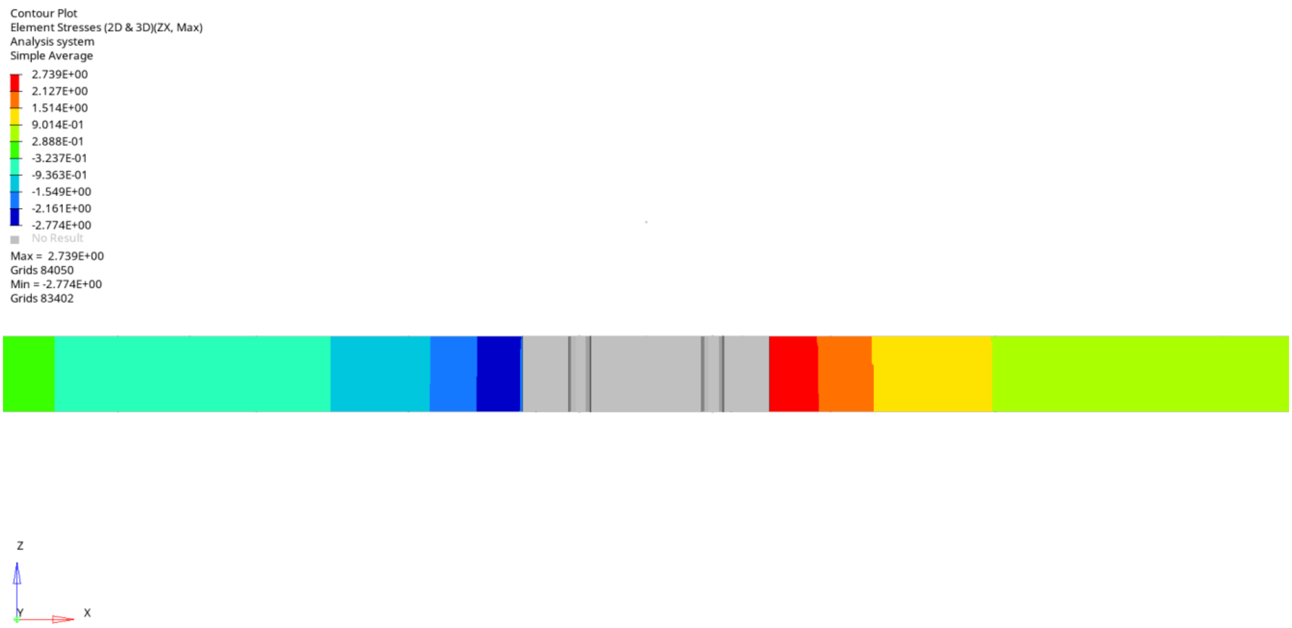

Baseline model - CFRP upper ply Plots:

The ply post processing usually is made by using a Failure Criteria, that in this case follows the Tsai-Wu formulation. One denotes the Tsai-Wu the number a such that:

- if a < 1: no ply rupture occurs;
- if a > 1: rupture occurs in the ply considered.

- Ply1 composite failure according to Tsai-Wu criteria:

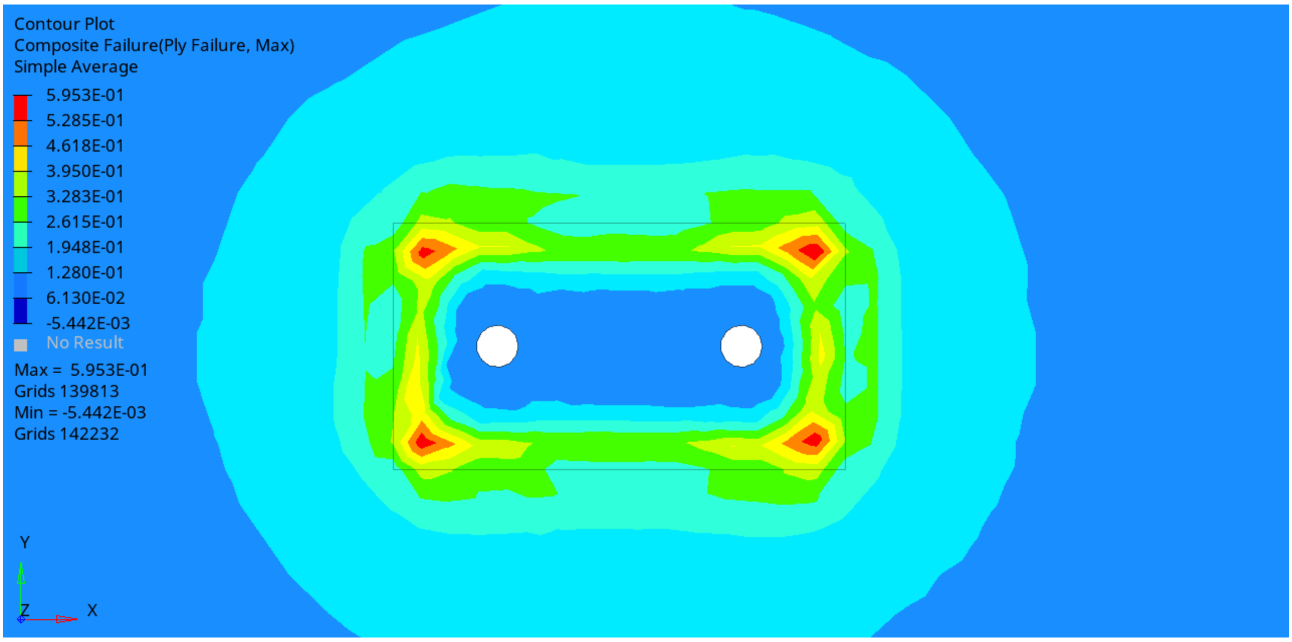

- Ply1 bond failure according to Tsai-Wu criteria:

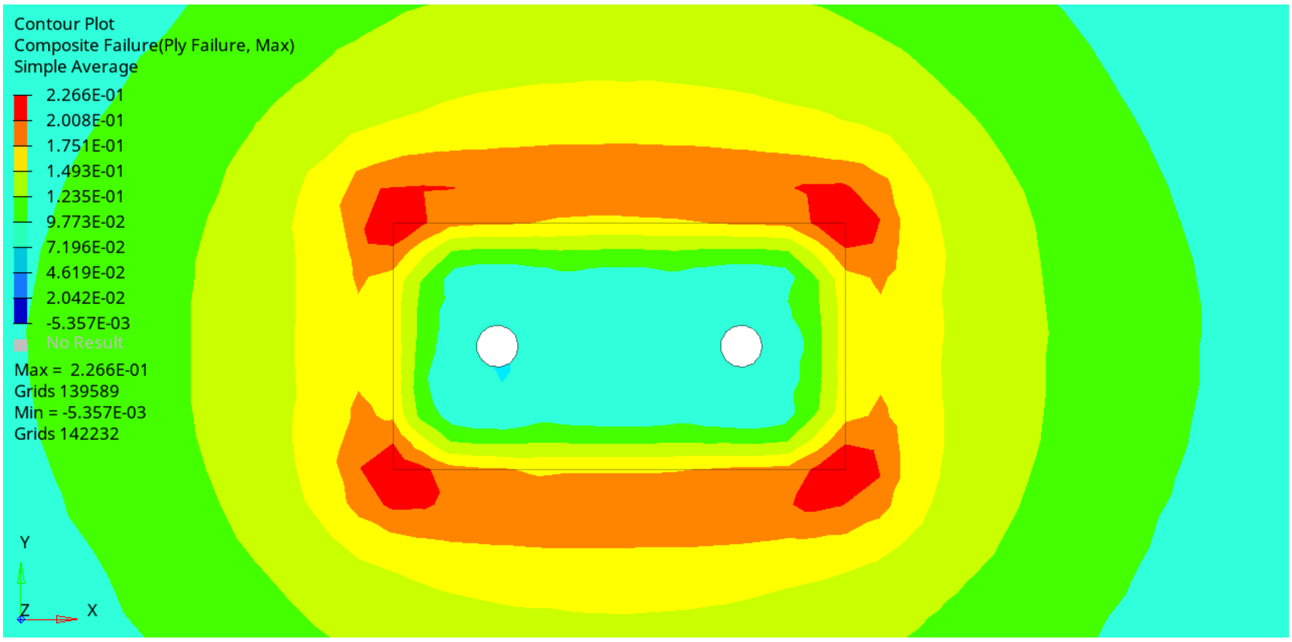

Baseline model - CFRP lower ply Plots:

- Ply 2 composite Failure according to Tsai-Wu criteria:

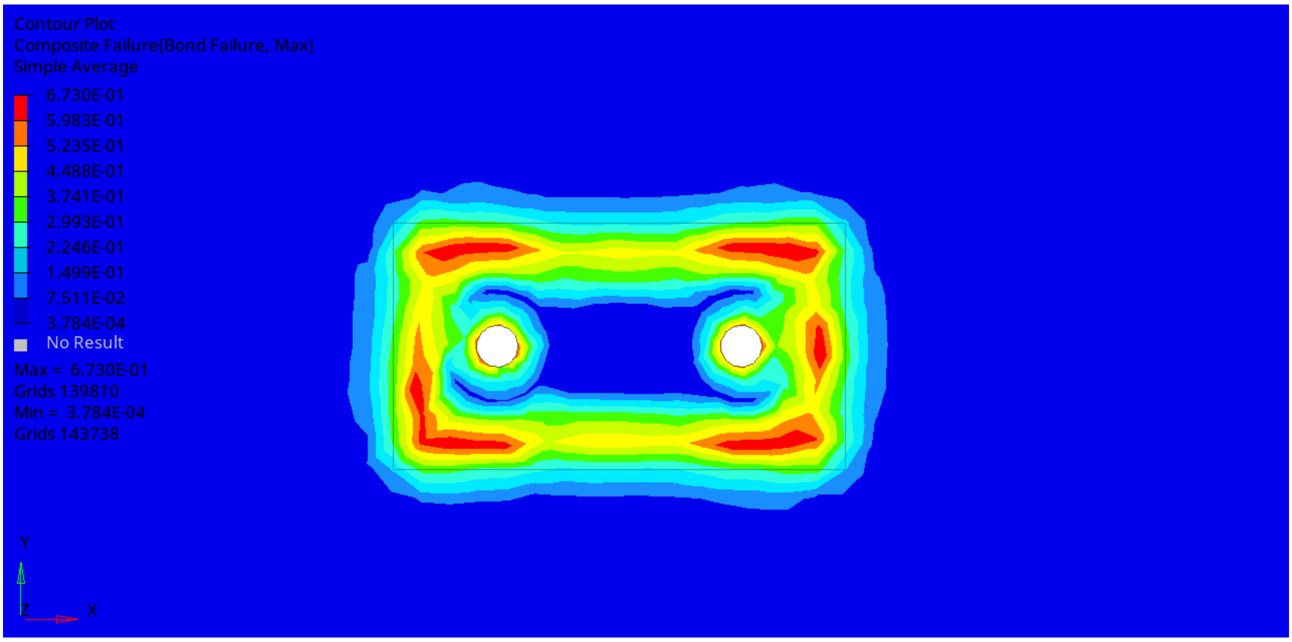

- Ply 2 Bond Failure according to Tsai-Wu criteria:

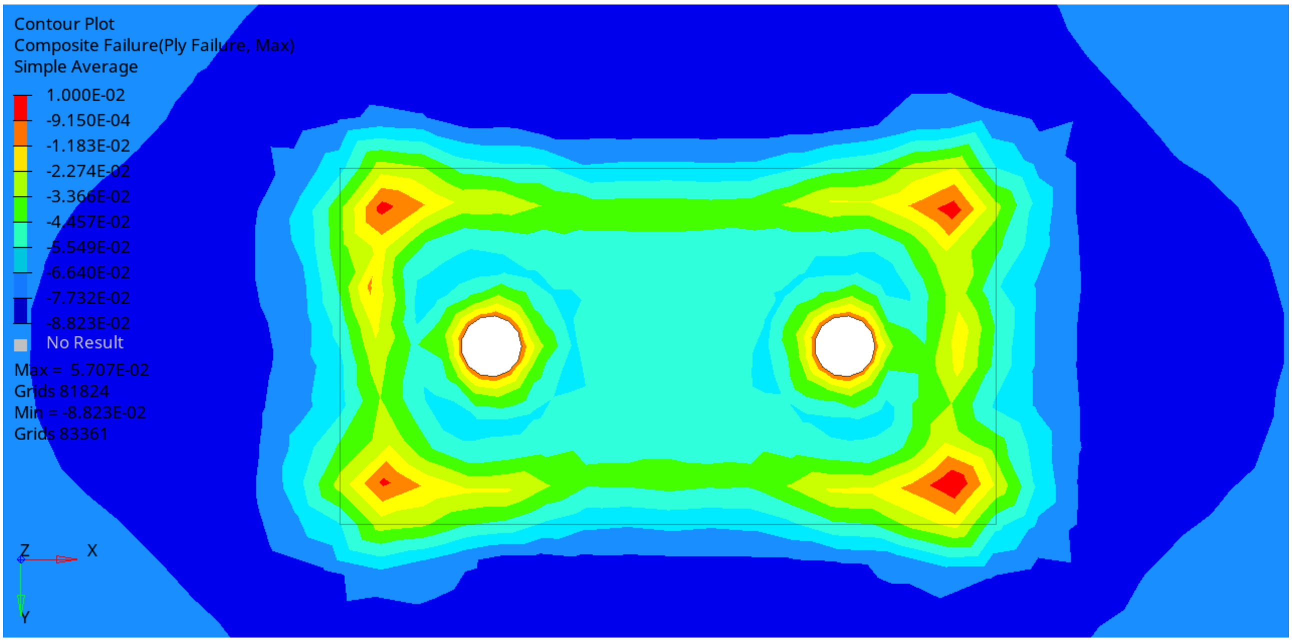

5.2. Case study 1 – Squadracorse insert with potting

The following case study is an improvement of the baseline model. A connection between the insert and the honeycomb is introduced with a Potting compound. The potting allows a better transmission of the tangential shear stress and avoid tensile and compress peak in the insert-core boundary nearby upper and lower ply (see Honeycomb plot of the Baseline model).

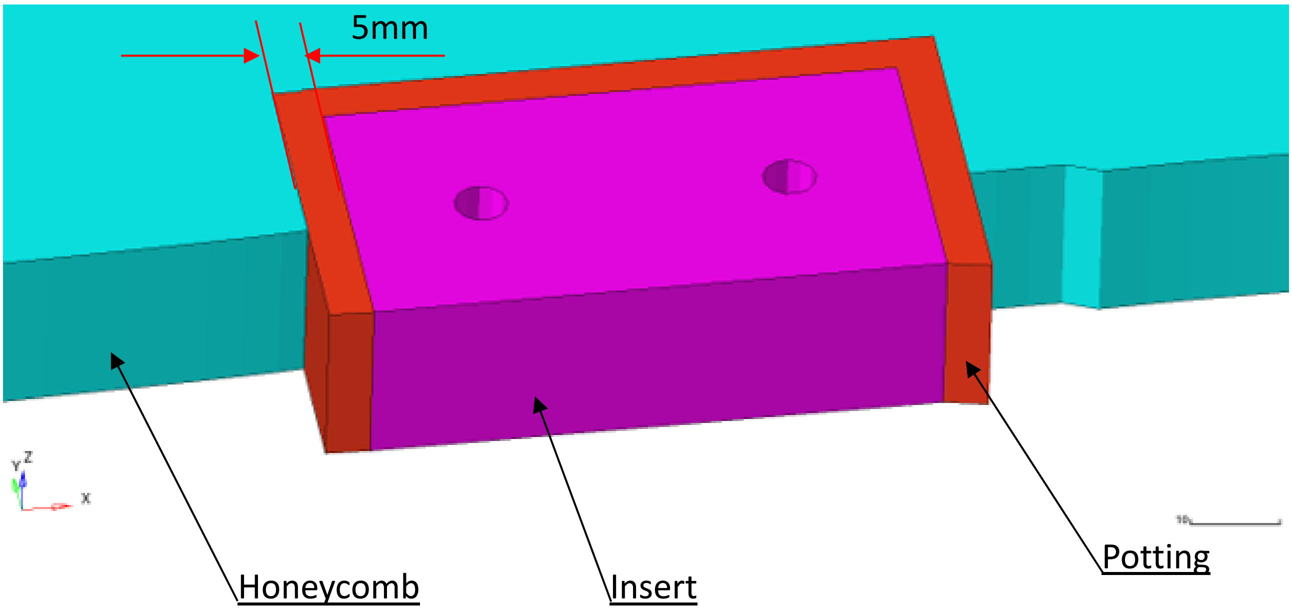

Material data according to CAP 4.3.3 and constraint iso 4.3.4. An overview of the Baseline model follows:

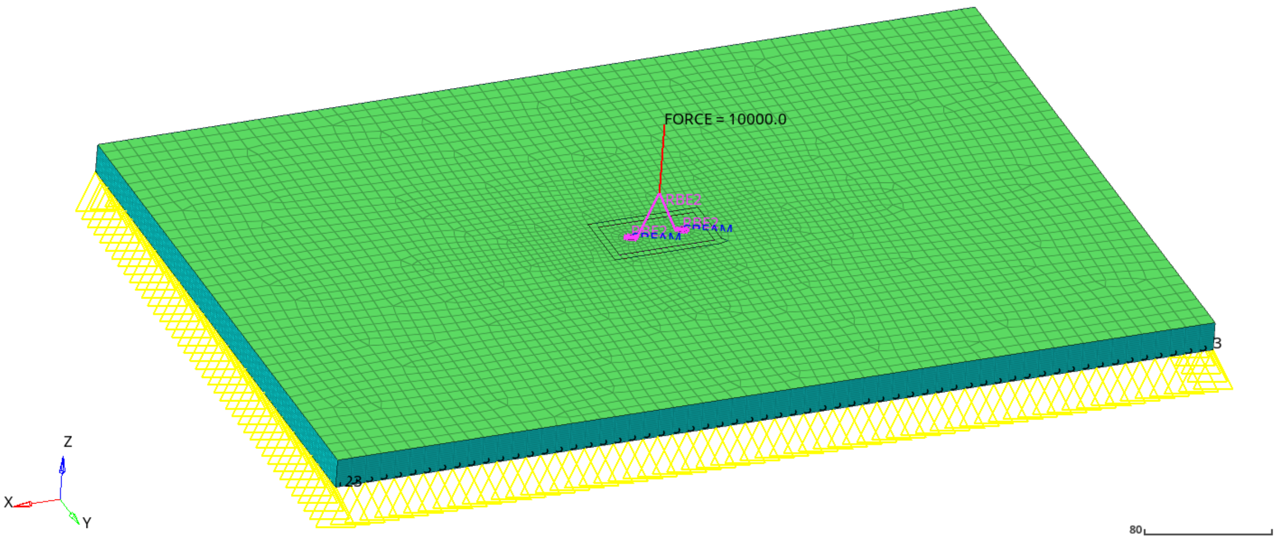

Case study 1 - Displacement field:

- Overall Z displacement of the sandwich panel Top view:

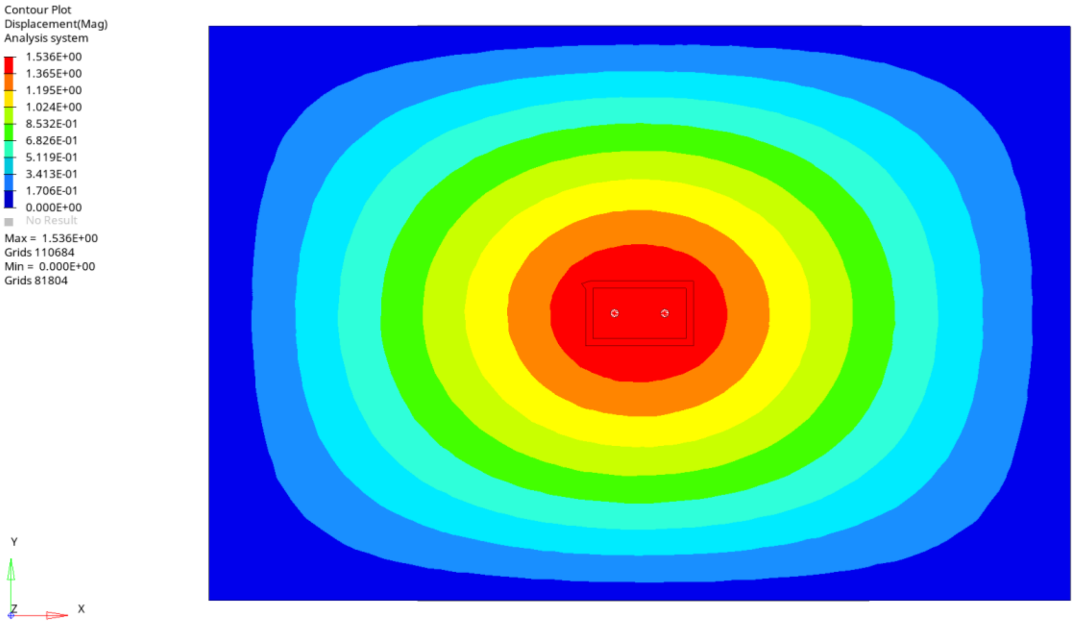

- Overall Z displacement of the sandwich panel cross section at Y=0, render multiplier x20:

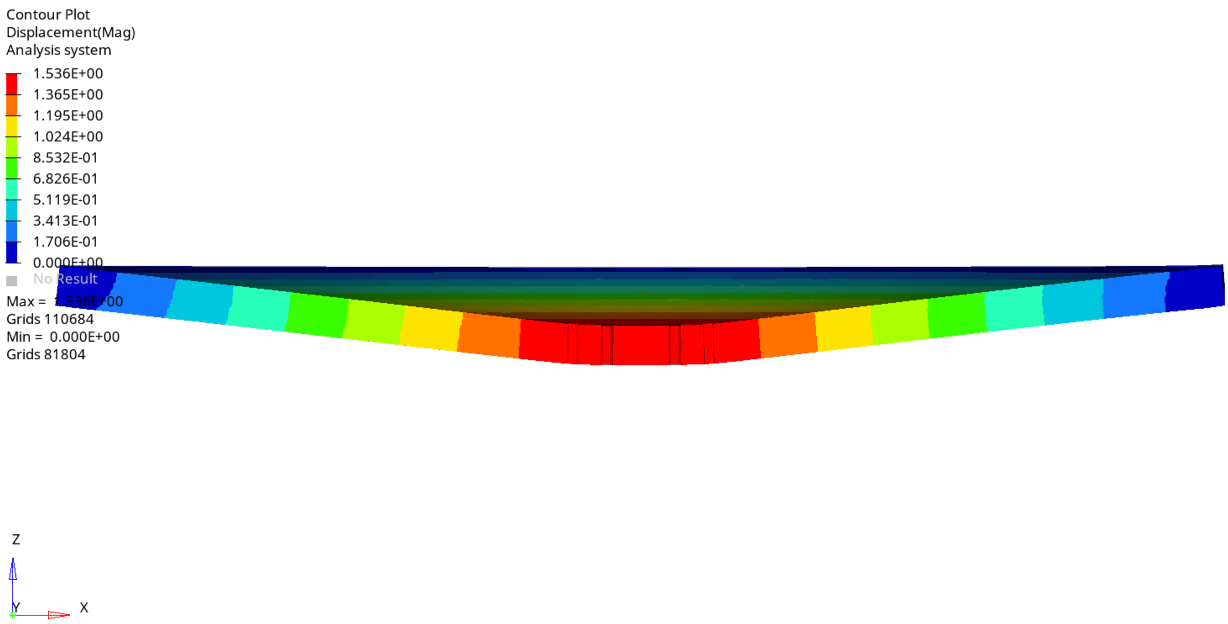

Case study 1 - Honeycomb plots:

- Honeycomb $\sigma_{ZZ,core}$: tensile/compressive stress

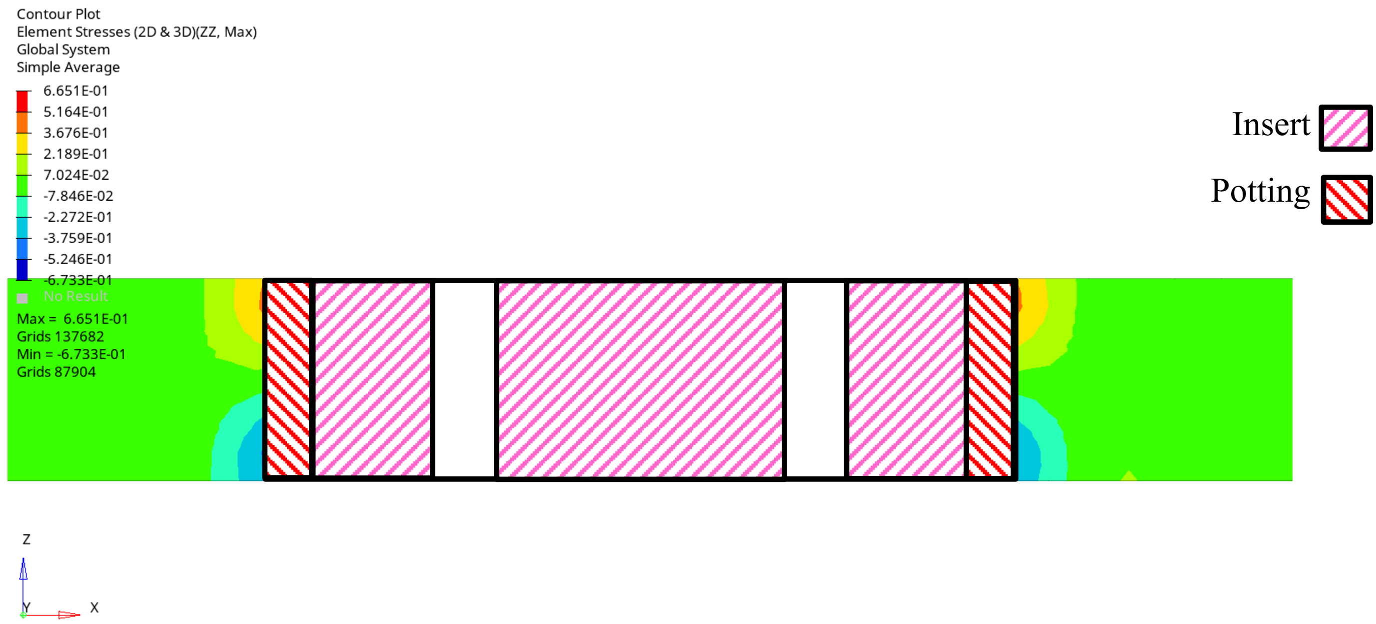

- Honeycomb $\tau_{ZX,core}$: transverse core shear stress

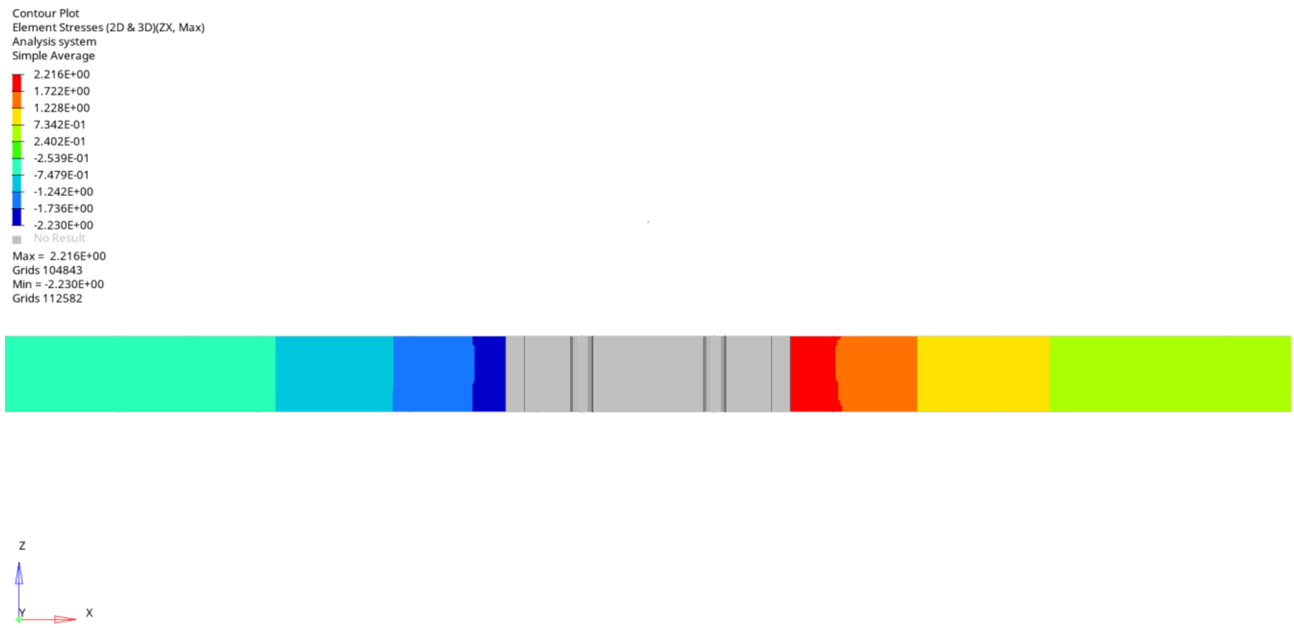

Case study 1 - Potting Plots:

- Potting $\sigma_{ZZ,core}$: tensile/compressive stress

- Potting $\tau_{ZX,core}$: transverse core shear stress

Case study 1 - CFRP upper ply Plots:

The ply post processing usually is made by using a Failure Criteria, that in this case follows the Tsai-Wu formulation. One denotes the Tsai-Wu the number a such that:

- If a < 1: no ply rupture occurs;
- If a > 1: rupture occurs in the ply considered.

- Ply1 composite failure according to Tsai-Wu criteria:

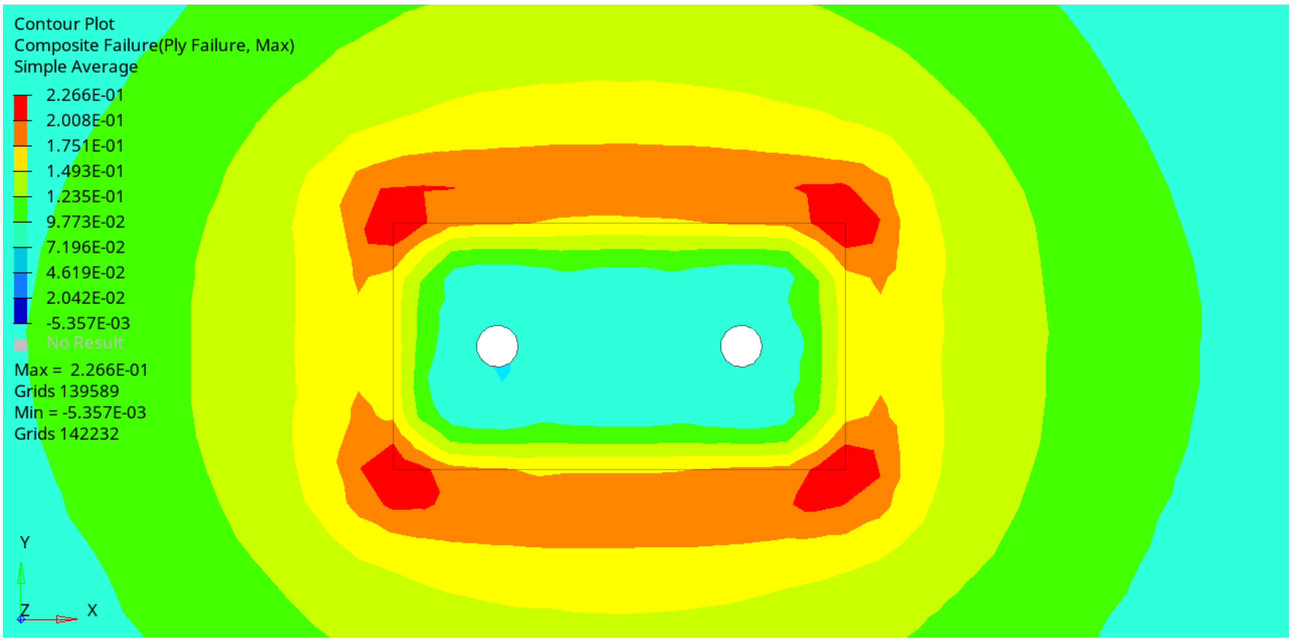

- Ply1 bond failure according to Tsai-Wu criteria:

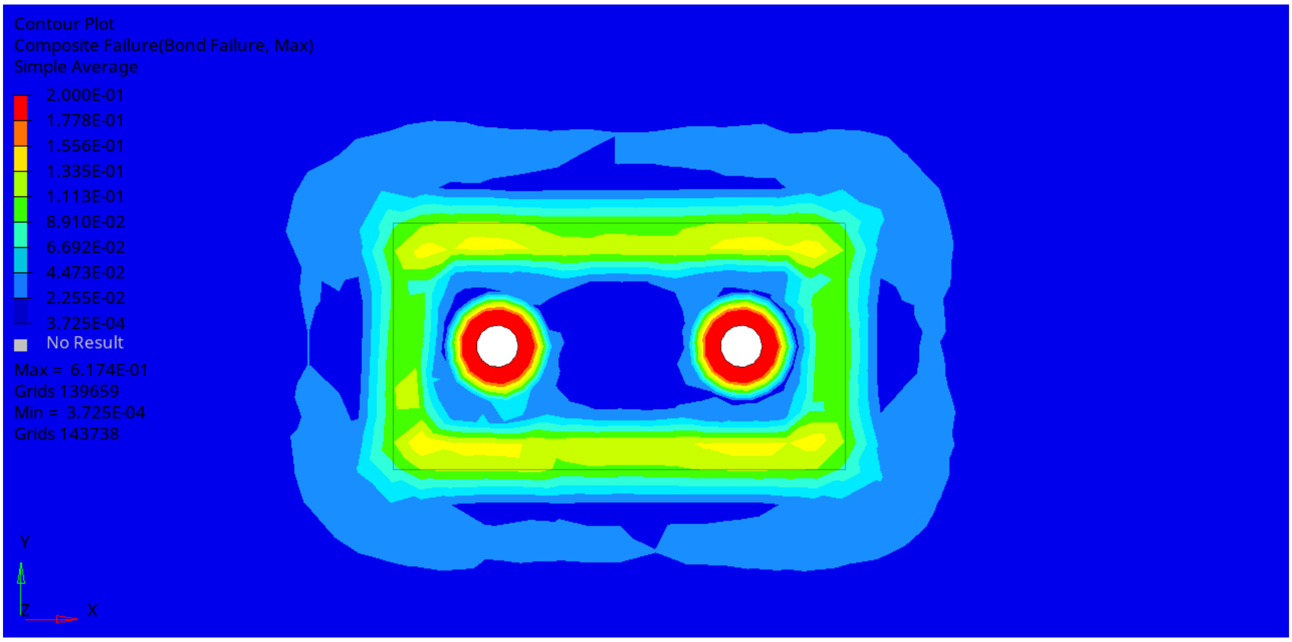

Case study 1 - CFRP lower ply Plots:

- Ply 2 composite failure according to Tsai-Wu criteria:

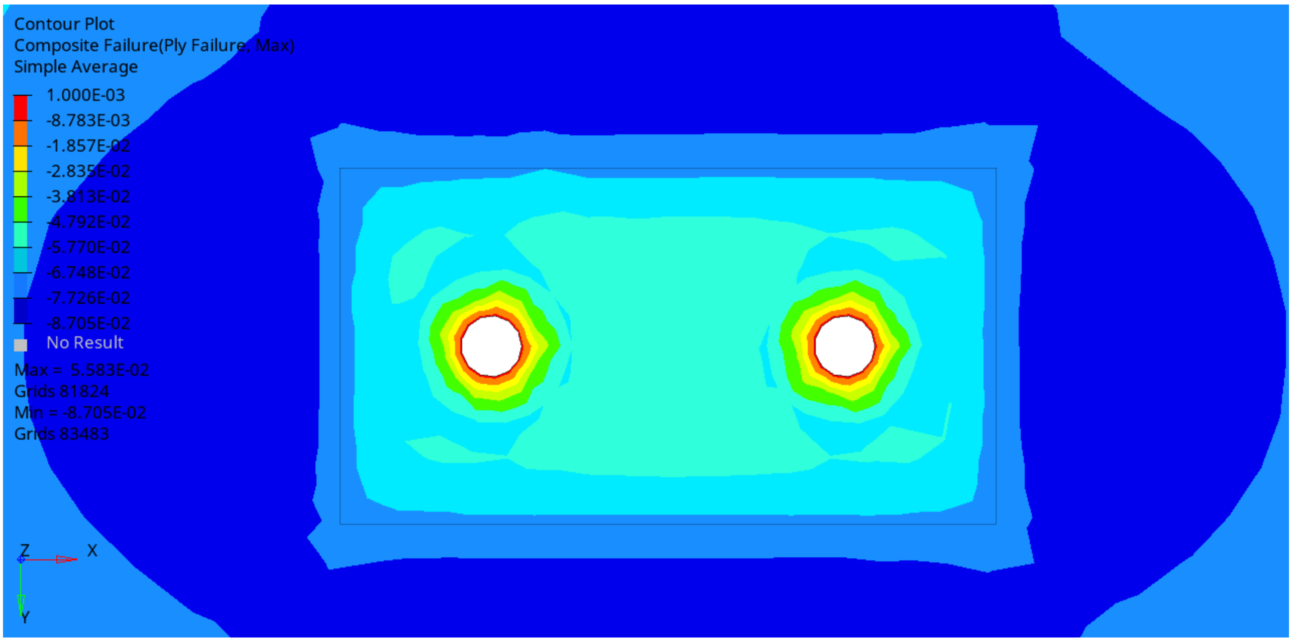

- Ply 2 bond failure according to Tsai-Wu criteria:

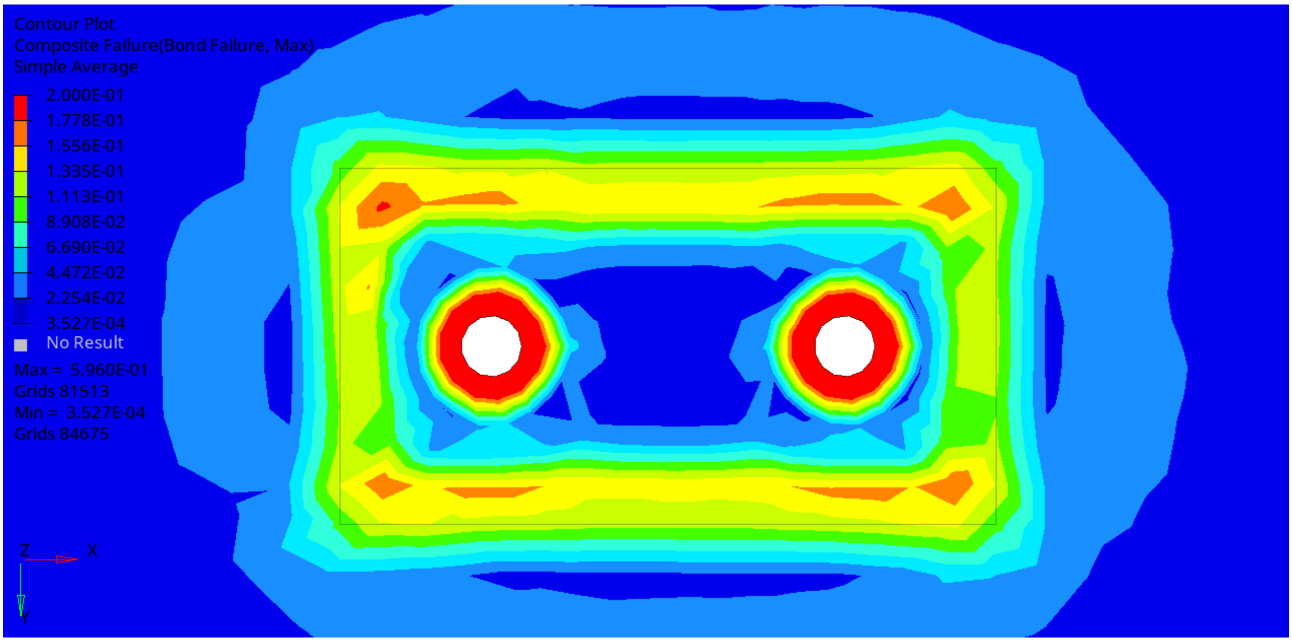

5.3. Case study 2 – advanced insert

The Case study 2 geometry is a step further in the insert design. The single block present in the Baseline model and Case Study 1 has been left for two distinctive inserts, one for each bolt of the suspension bracket. A full description of the modelling will follow.

5.3.1. Case study 2 - Pre-processing

A total number of 1829 2d elements has been used for each ply modelling of types:

- CTRIA3;
- CPENTA4.

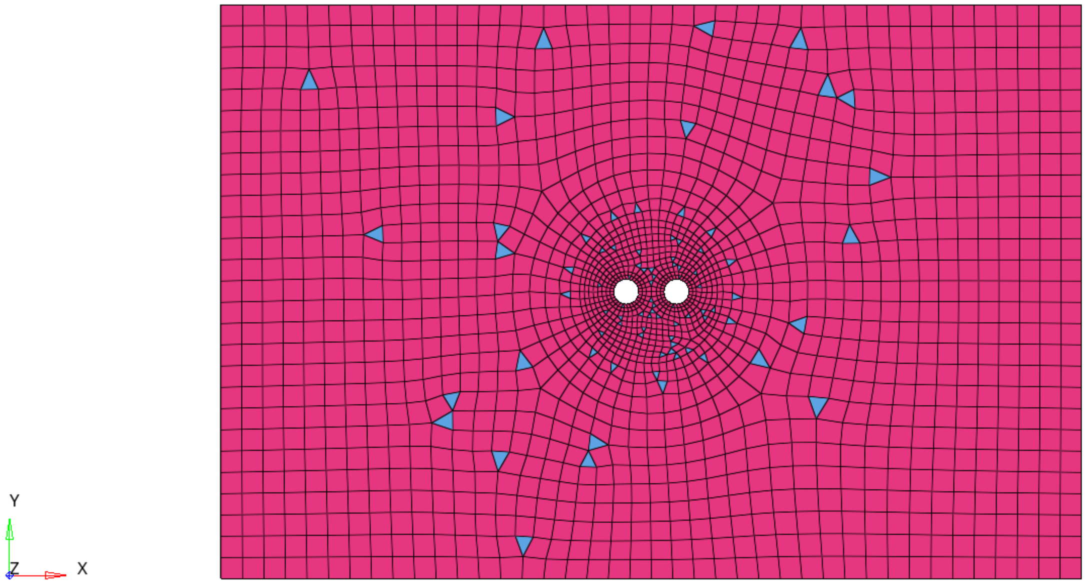

Legenda:

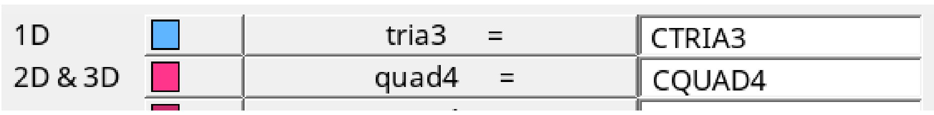

1D		tria3 =	CTRIA3
2D & 3D		quad4 =	CQUAD4

25.753 3d elements has been used for Inserts, potting and core elements, of type:

- HEX8;
- PENTA6.

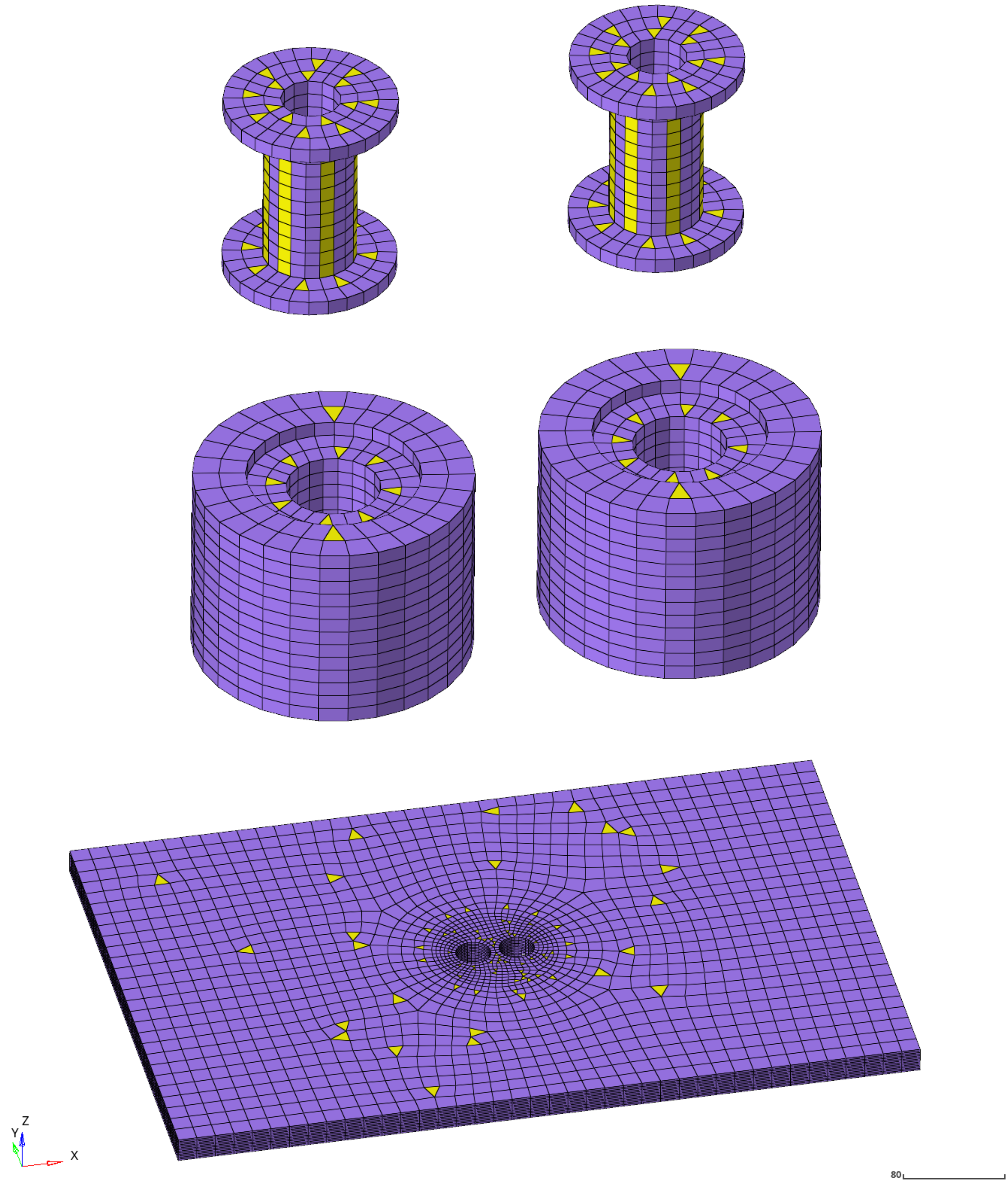

Legenda:

	penta6 =	CPENTA
	hex8 =	CHEXA

1d elements has been used for Bolts and Suspension bracket modelling:

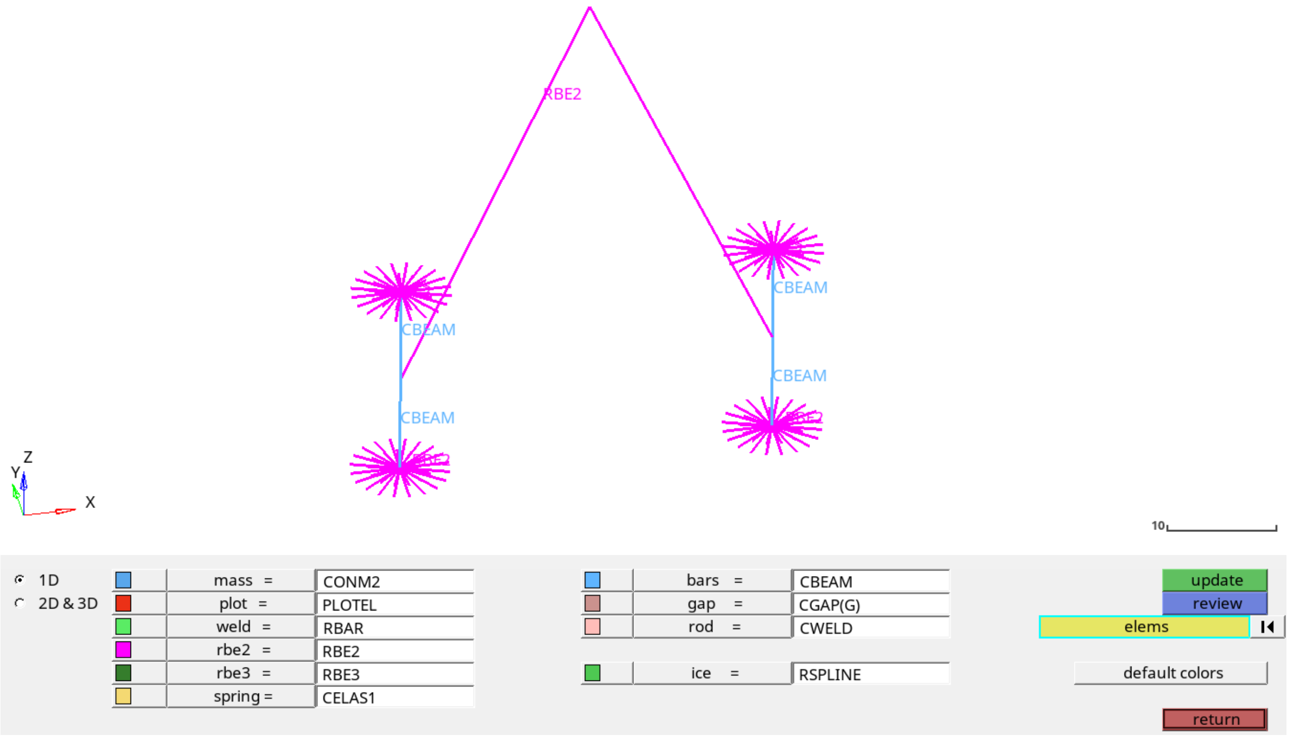

Material data according to CAP 4.3.3 and constraint iso 4.3.4. An overview of the Baseline model follows:

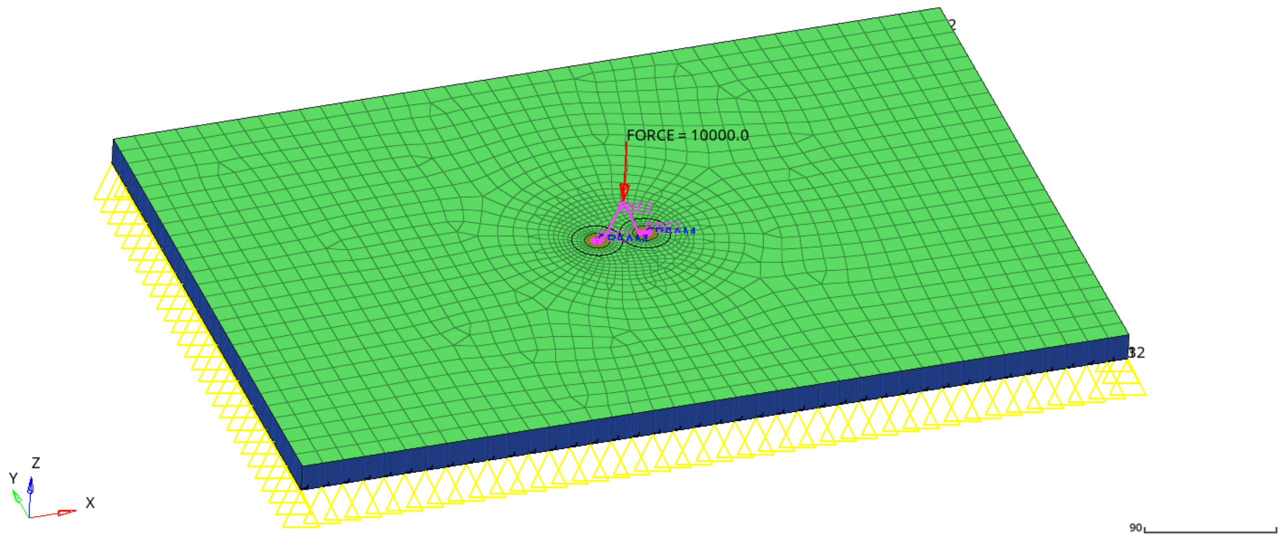

5.3.2. Case Study 2 – Post processing

Case study 2 - Displacement field:

- Overall Z displacement of the sandwich panel top view:

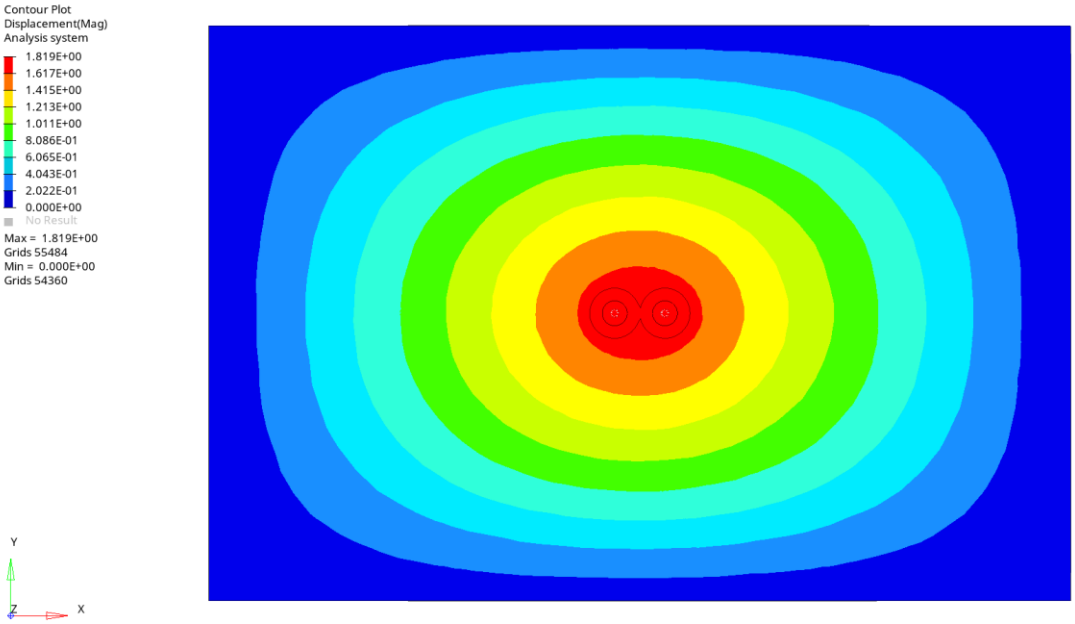

- Overall Z displacement of the sandwich panel cross section at Y=0, render multiplier x20:

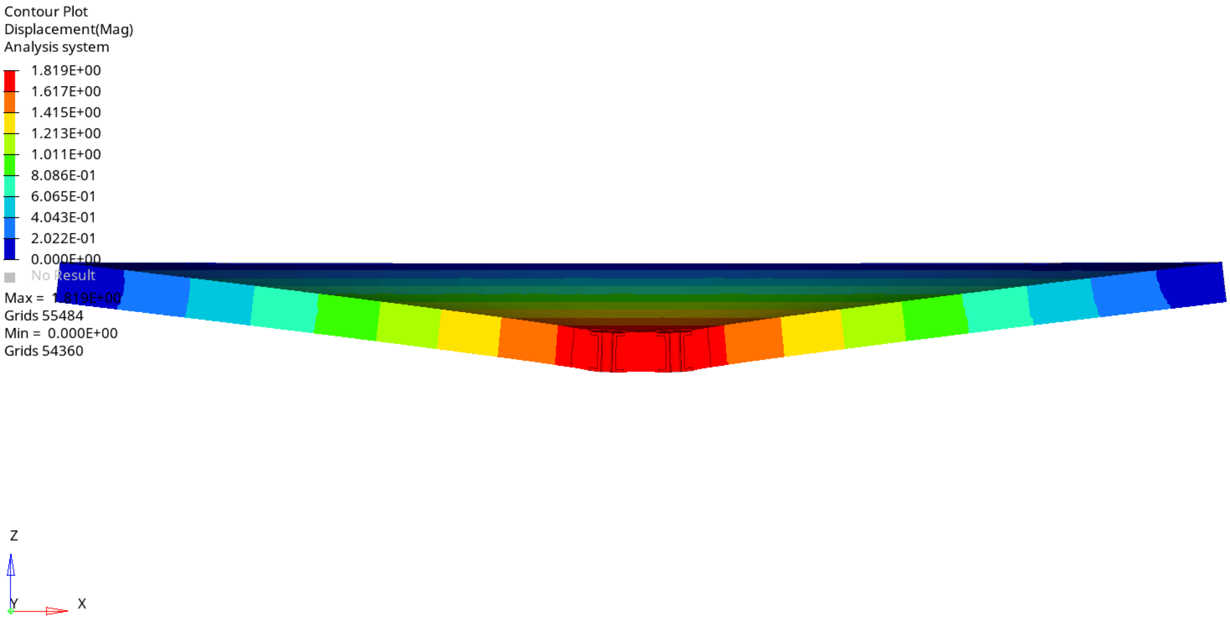

Case study 2 - Honeycomb plots:

- Honeycomb $\sigma_{ZZ,core}$: tensile/compressive stress

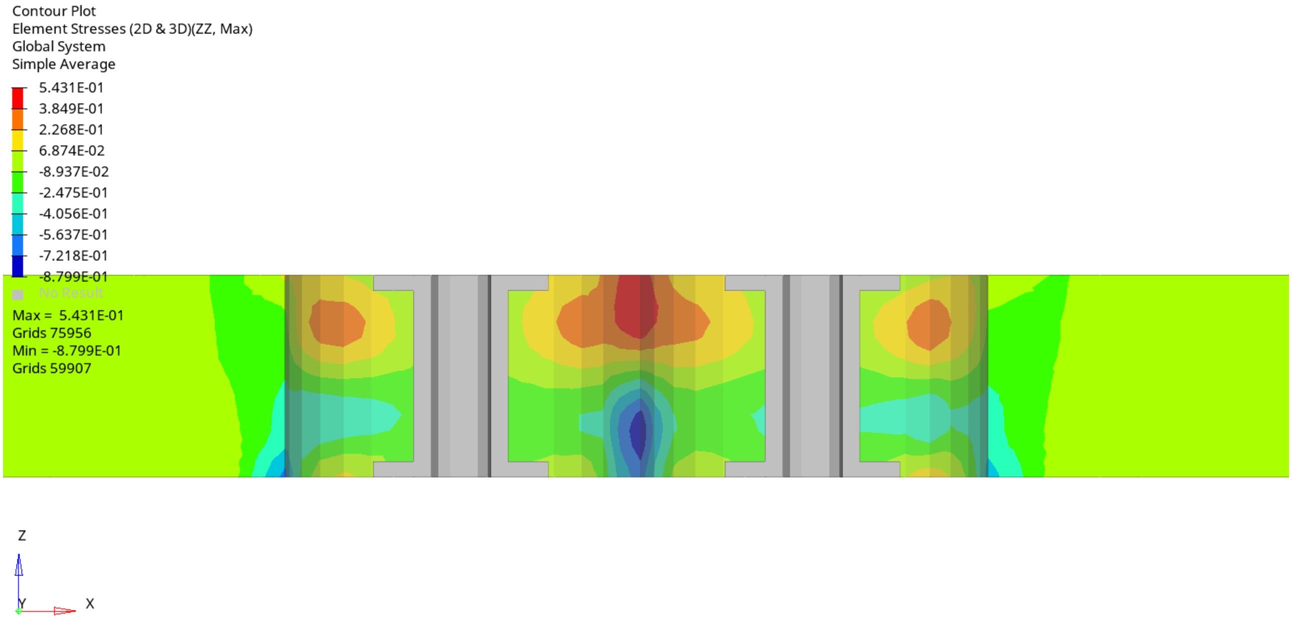

- Honeycomb $\tau_{ZX,core}$: transverse core shear stress

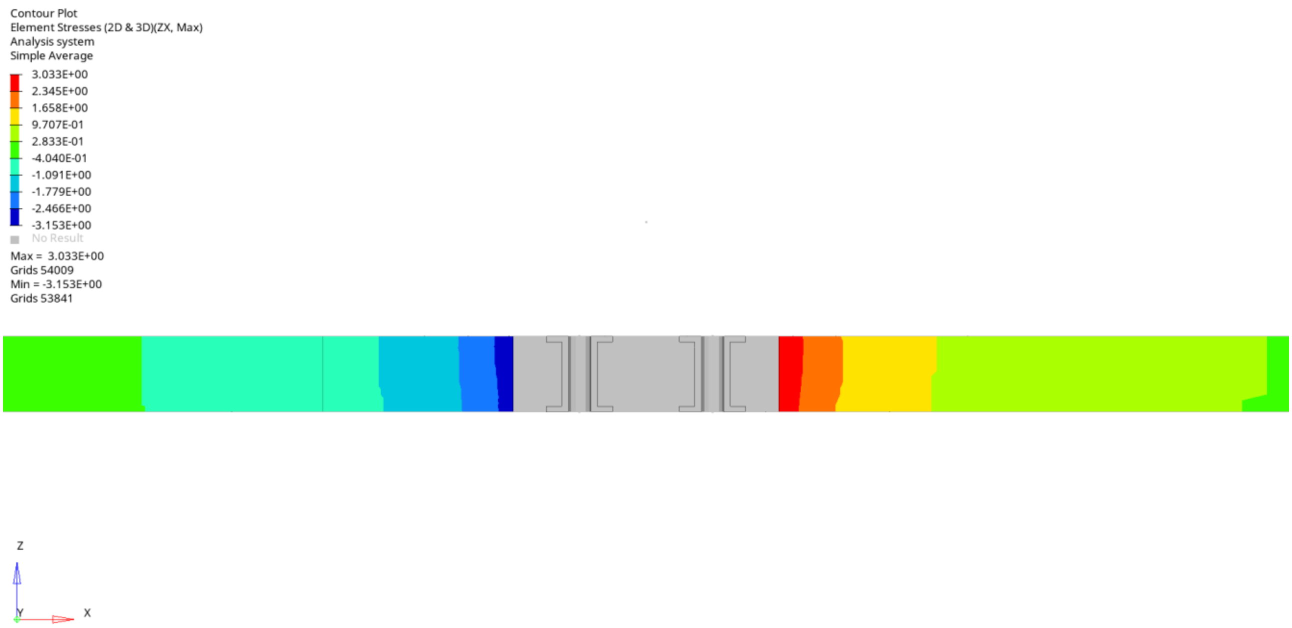

Case study 2 - Potting Plots:

- Potting $\sigma_{ZZ,core}$: tensile/compressive stress

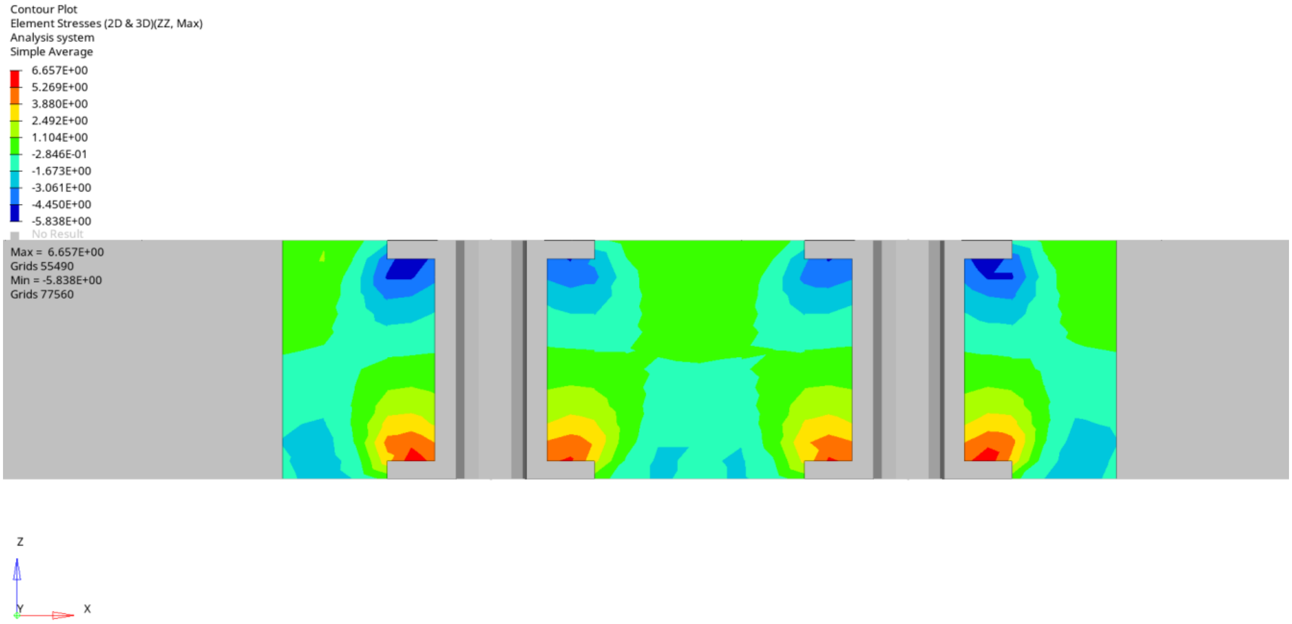

- Potting $\tau_{ZX,core}$: transverse core shear stress

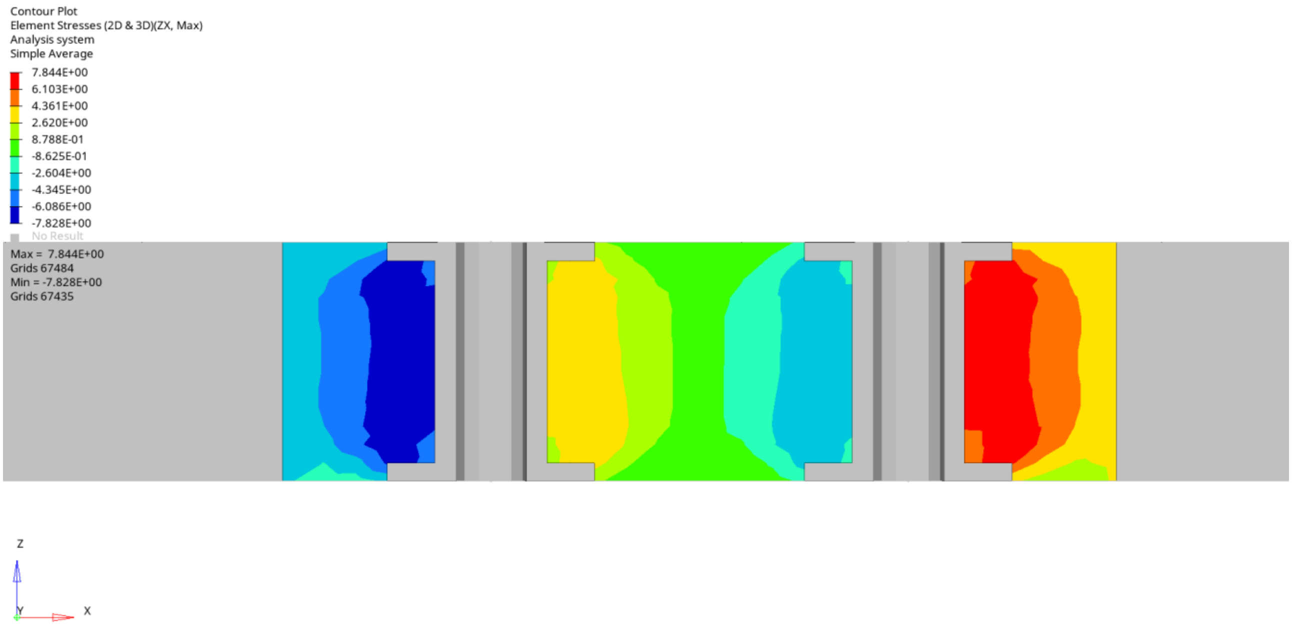

Case study 2 - CFRP upper ply Plots:

The ply post processing usually is made by using a Failure Criteria, that in this case follows the Tsai-Wu formulation. One denotes the Tsai-Wu the number a such that:

- If $a < 1$: no ply rupture occurs;
- If $a > 1$: rupture occurs in the ply considered.

- Ply1 composite failure according to Tsai-Wu criteria:

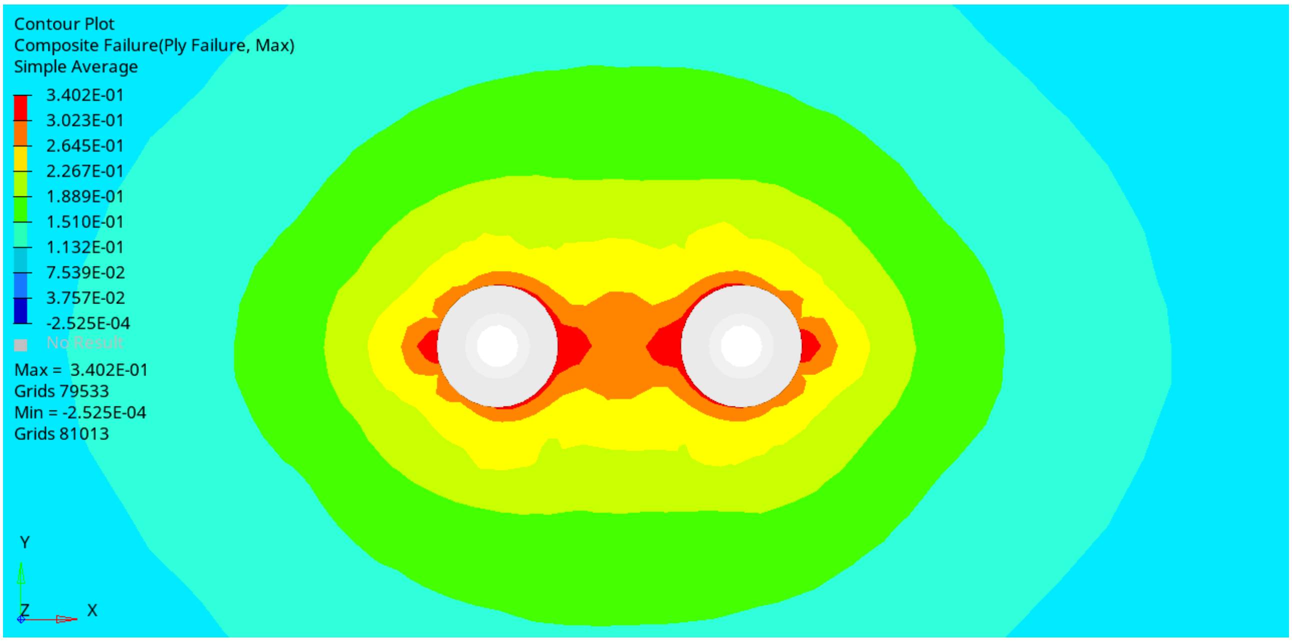

- Ply1 bond failure according to Tsai-Wu criteria:

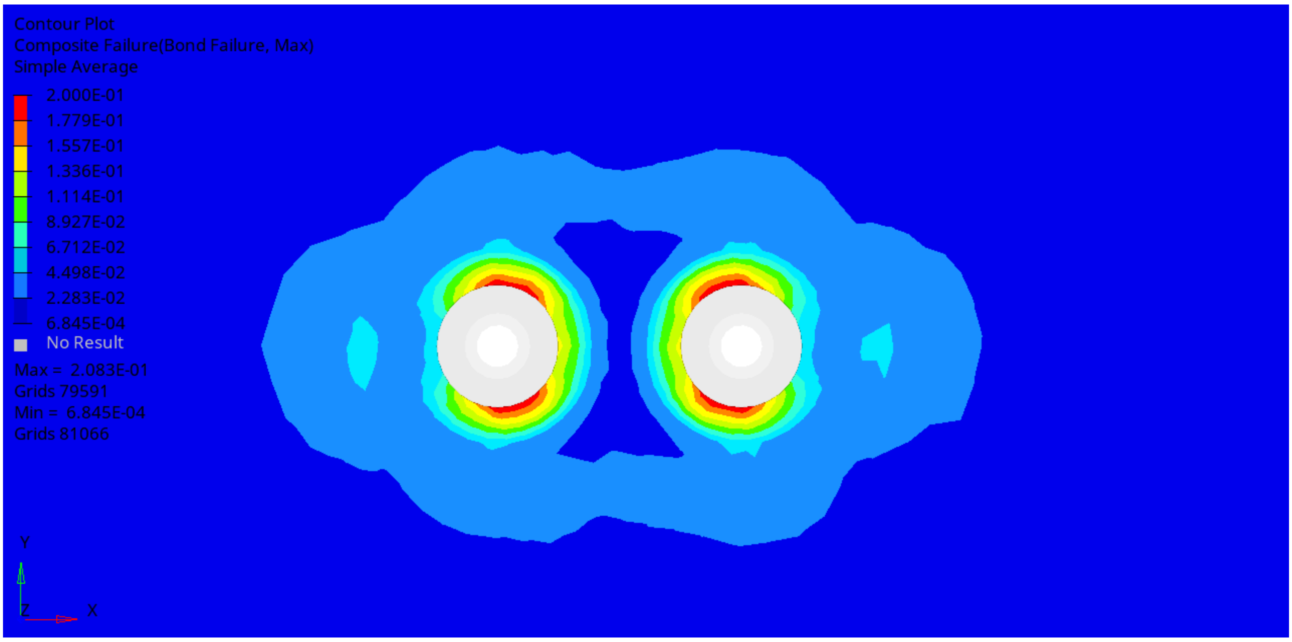

Case study 2 - CFRP lower ply Plots:

- Ply 2 composite failure according to Tsai-Wu criteria:

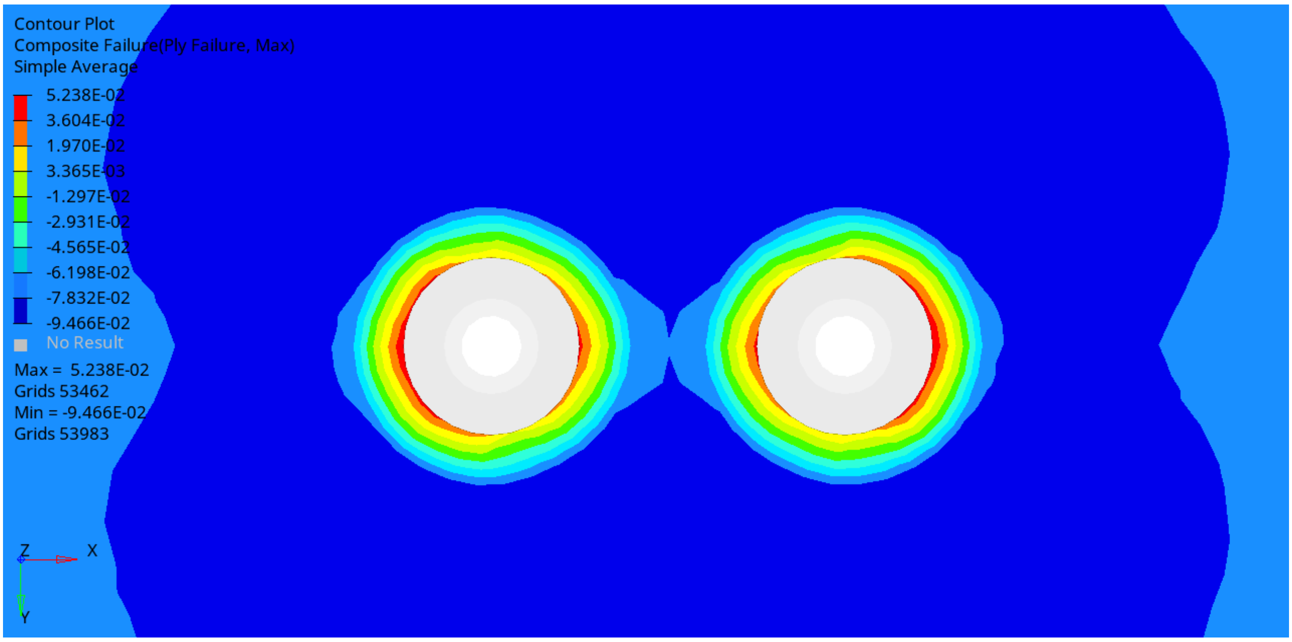

- Ply 2 bond failure according to Tsai-Wu criteria:

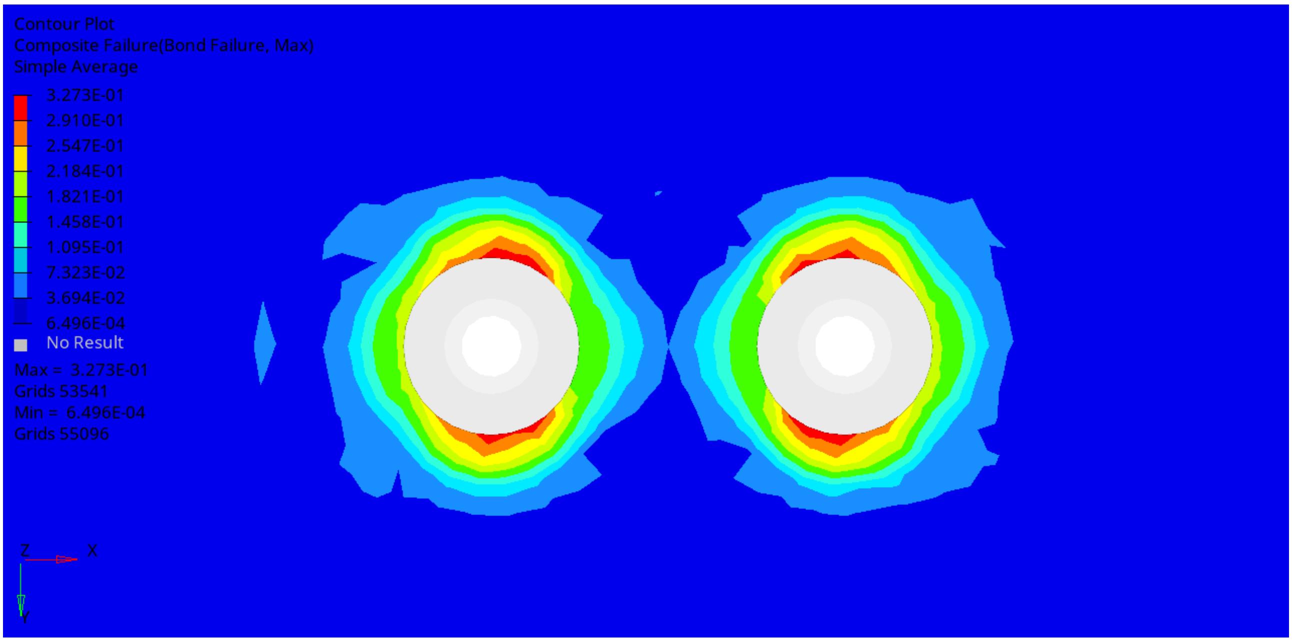

5.4. Suspension insert application case results overview

The following discussion is a prediction of the suspension insert behavior based on FEM linear elastic models. In order to properly evaluate the insert failure loads and the current safety margins, FEM Non-linear Explicit analysis are required, not part of this paper.

It's fundamental to sum-up the post processing of the FEM models by comparing the contour results with the material limits. First of all, core and potting material results:

DATA		Baseline Through the thickness insert block w/o potting		Case study 1 SC with potting		Case study 2 Through the thickness insert with Potting		Reference Value
		[MPa]	Margin	[MPa]	Margin	[MPa]	Margin	[MPa]
Core	Sigma ZZ	9.7	0.5	0.7	7.4	0.5	10.4	5.2
		-9.2	0.6	-0.7	7.4	-0.8	6.5	-5.2
	TAU ZX	2.7	1.2	2.2	1.5	3.0	1.1	3.2
	TAU ZY	2.3	1.2	2.0	1.4	2.5	1.1	2.7
Potting	Sigma ZZ	-	-	0.9	44.7	6.5	5.8	38.0
		-	-	-1.0	48.0	-6.0	8.0	-48.0
	TAU ZX	-	-	3.4	10.1	7.8	4.4	34.5
		-	-	-3.5	9.9	-7.8	4.4	-34.5

Secondly, ply failure criteria results. In this case the Tsai-Wu formulation has been adopted. One denotes the Tsai-Wu the number a such that:

- if a < 1: no ply rupture occurs;
- if a > 1: rupture occurs in the ply considered.

DATA		Baseline Through the thickness insert block w/o potting		Case study 1 SC with potting		Case study 2 Through the thickness insert with Potting	
		Tsai-Wu Failure criteria	Margin	Tsai-Wu Failure criteria	Margin	Tsai-Wu Failure criteria	Margin
Ply 1	Ply Failure	0.6	1.7	0.2	5.0	0.4	2.9
	Bond Failure	0.7	1.5	0.2	5.0	0.2	5.0
Ply 2	Ply Failure	0.1	20.0	0.1	20.0	0.1	20.0
	Bond Failure	0.8	1.3	0.2	5.0	0.3	3.3

The transverse load transmission is critical in the insert-honeycomb interface. Looking at the **Baseline** model results, the tensile/compressive status of the honeycomb (Sigma ZZ) is highly over the material limits, because of the external load is transmitted along the sandwich panel only via the higher and lower CFRP plys in the area of the insert perimeter. Negative results are visible also in the Plys failure criteria, the latter parameter gives us the indication of a wrong design, and highlight the need of a better transverse load distribution.

In the **Case Study 1**, there is dramatic reduction of tensile/compressive stress and also a reduction of tangential shear stress in both direction ZX and ZY (respectively honeycomb L and W directions). Similar reductions are visible in the CFRP plys. Relevant margins are visible for potting, Ply 1 and Ply 2 components. The potting material introduction shows a general improvement in the insert assembly load response and give us the possibility to optimize the alluminium insert shape, looking for weight reduction and a reduction of the high margins, that are index of over-design.

The **Case Study 2** exploit the potting compound in higher way and reduce the potting margin up to 90% with respect to case study 1, higher shear stresses are visible in the core material and CFRP plys. Relevant weight reduction is possible with this solution.

Displacements and weight considerations are possible by knowing max panel deflections and material density. Case study 1 shows a worse stiffness/weight radio with respect to Baseline but it is a reliable solution since no core failure occurs. Case study 2 is the best solution for both reliability and weight to stiffness ratio. It follows the compete overview:

	Baseline	**Case study 1**	**Case study 2**	DATA
	Through the thickness insert block w/o potting	SC with potting	Through the thickness insert with Potting	Unit
Displacement	1.67	1.54	1.82	mm
Mass	57	91	52	g
Stiffness	5988	6494	5495	kN/mm
Stiffness/weight	103	71	105	kN/mm/g

6. Conclusions

The approach used by the SquadraCorse Formula SAE team during the **SCXV insert design**, was the use of a through the thickness insert embedded in the sandwich panel, via cold bonding without core connection. For what regards the calculation method, a lack of information was present especially for the honeycomb behaviour prediction, nor sigma or tau max stress has been verified.

The insert capability evaluation based on the **Anti-plane Theory analytical method**, takes into account the use of cylindrical insert with potting connection to the honeycomb core. The analytical method is a quick and powerful tool: it can provide reliable result for the failure load evaluation of a single insert and, with the use of proximity coefficient, the failure load of set of inserts loaded in the same or in the opposite directions. This method can be adopted more in general for all monocoque connections where there is no requirement in stiffness determination, and where the hypothesis of the antiplane theory can be applied.

The **Finite Elements Method** shows high accuracy and versatility. Any type of geometry can be simulated and extensive information regards the insert behaviour can be retrieved. The cons of FEM analysis lie in its complexity and calculation time with respect to analytical ones.

For what regards the **suspension insert application case**, the SquadraCorse <u>Baseline</u> insert design has been evaluated as not OK due to the honeycomb overloading. The Baseline insert concept exploited in a wrong way the insert assembly capability by loading solely the CFRP plys surrounding the aluminium insert with an out-of-plane loads. This yield to high tensile/compressive stress in the honeycomb that exceed the material properties; stress concentrations are localized in the honeycomb facing the insert surface and in contact with the outer ply. Improvement of the Baseline model are present in the <u>Case study 1</u>, by connecting the insert to the honeycomb material with the potting compound; in this scenario the insert assembly lie in safety conditions but with relevant weight increase. Finally, <u>Case Study 2</u> improves the insert performance by increasing the specific stiffness of the Baseline case while respecting also the material max allowable stresses.

7. References:

- **European Cooperation for Space Standardization -** Insert design handbook ECSS-E-HB-32-22A;
- **O.T. Thompson and F. L. Matthews -** Load attachment for honeycomb panels in racing cars;
- **O.T. Thompson -** Sandwich plates with through-the-thickness and ‘fully potted’ inserts: evaluation of differences in structural performance;
- **O.T. Thomsen and W. Rits -** Analysis and design of sandwich plates with inserts;
- **Johannes Wolffa, Marco Bryschb, Christian Hühnea -** Validity check of an analytical dimensioning approach for potted insert load introductions in honeycomb sandwich panels;
- **Elena Bozhevolnayaa,1, Anders Lyckegaarda, O.T. Thomsena, Vitaly Skvortsov -** Local effects in the vicinity of inserts in sandwich panels;
- **D. Gay, S. V. Hoa, S. W. Tsai -** Composite Materials Design and Applications.

8. Appendix I - Vehicle dynamics input load for suspension attachment design.

Vehicle coordinate system according to the figure:

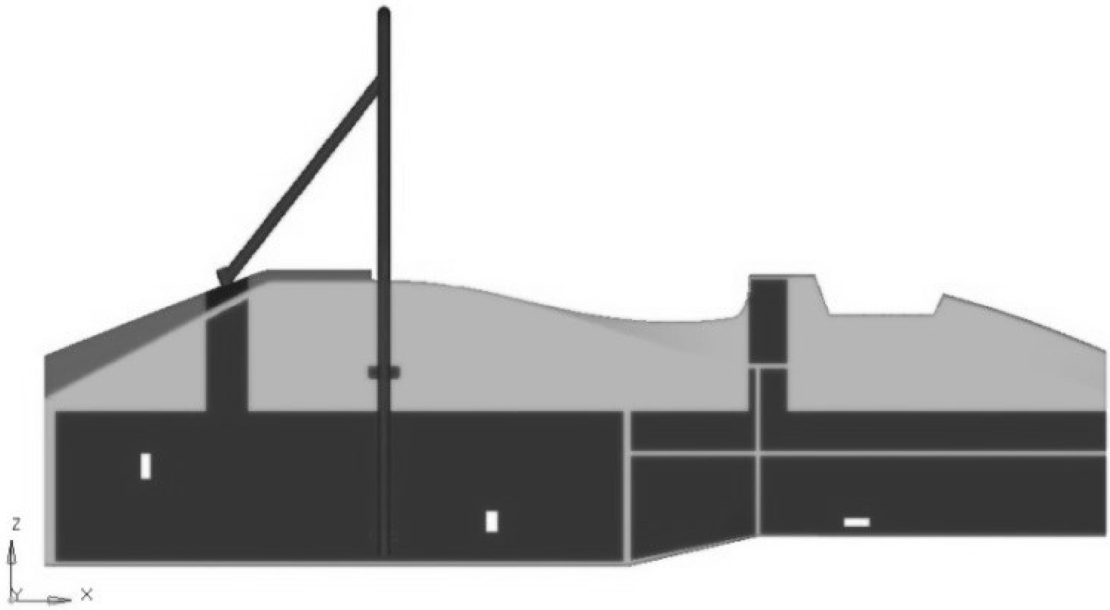

Legenda	
LCA F	Lower contro Arm
UCA O	Upper control Arm
Push I	Pushroad
Upright	-
Hub	-
Tie I	Tie rod
ARB	Antirollbar
Rocker damper joint	-
Rocker pivot	-

Sweep test front	Fx	Fy	Fz
LCA F	-465	4389	967
LCA R	0	1514	343
LCA O	465	-5912	-1316
UCA F	-809	-360	-29
UCA R	0	-1550	-122
UCA O	809	1486	-172
Push O	0	-424	-322
Push I	0	424	321
Upright	754	-3000	-1240
Hub	-	-	-
Tie O	-610	1682	286
Tie I	610	-1682	-297
ARB droplink left	65	295	-9
ARB droplink right	-60	-296	-6
Arb attachment	125	591	-33
Rocker damper joint	0	871	5
Rocker pivot	-57	-84	695

Sweep test rear	Fx	Fy	Fz
LCA F	a	1975	400
LCA R	0	3003	256
LCA O	520	-4168	-767
UCA F	909	-1602	272
UCA R	0	-2364	269
UCA O	704	1655	-500
Push O	0	-1319	-845
Push I	0	1319	844
Upright	1381	-2657	-1261
Hub	-	-	-
Tie O	50	-333	-2.5
Tie I	-50	333	-8.7
ARB droplink left	-32	-162	-13
ARB droplink right	-32	-163	-7
Arb attachment	-63	-322	-33
Rocker damper joint	0	953	-15
Rocker pivot	-32	217	849

Acceleration test front	Fx	Fy	Fz
LCA F	32	3150	342.5
LCA R	0	1707.8	183.6
LCA O	-32.6	-4858	-532
UCA F	-25	-1533.3	68.6
UCA R	0	-952	42.88
UCA O	25	1727.2	-656.2
Push O	-0.3	-757.9	-542.7
Push I	0.3	757.9	541.5
Upright	-92.5	-2890.6	-1184
Hub	-	-	-
Tie O	-84.73	240	11.35
Tie I	84.73	-240	-22.7
ARB droplink left	in this test the arb doesn't work		
ARB droplink right			
Arb attachment			
Rocker damper joint	0	689.96	9.5
Rocker pivot	1.58	65.94	296.3

acceleration_test Rear	Fx	Fy	Fz
LCA F	-1046	1144	223
LCA R	0	-1171	-103
LCA O	1046	26	-126
UCA F	-1150	776	-173
UCA R	0	-2093	324
UCA O	1150	257	-834
Push O	0	-1059	-681
Push I	0	1059	680
Upright	2270	-193	-946
Hub	-	-	-
Tie O	72	477	20
Tie I	-72	477	-32
ARB droplink left	in this test the arb doesn't work		
ARB droplink right			
Arb attachment			
Rocker damper joint	0	876	-12
Rocker pivot	0	181	628

Brake front	Fx	Fy	Fz
LCA F	1060	-1365	28
LCA R	0	1323	36
LCA O	-1055	45	-70
UCA F	1570	-2344	297
UCA R	0	1181	-218
UCA O	-1569	-362	-1072
Push O	0	-1525	-991
Push I	0	1525	989
Upright	-2840	285	-1156
Hub	-	-	-
Tie O	-211	606	-7
Tie I	211	-606	-3
ARB droplink left	in this test the arb doesn't work		
ARB droplink right			
Arb attachment			
Rocker damper joint	0	1657	9
Rocker pivot	0	-131	970

BIT front	Fx	Fy	Fz
LCA F	32	3150	342.5
LCA R	0	1707.8	183.6
LCA O	-32.6	-4858	-532
UCA F	-25	-1533.3	68.6
UCA R	0	-952	42.88
UCA O	25	1727.2	-656.2
Push O	-0.3	-757.9	-542.7
Push I	0.3	757.9	541.5
Upright	-92.5	-2890.6	-1184
Hub	-	-	-
Tie O	-84.73	240	11.35
Tie I	84.73	-240	-22.7
ARB droplink left	in this test the arb doesn't work		
ARB droplink right			
Arb attachment			
Rocker damper joint	0	689.96	9.5
Rocker pivot	1.58	65.94	296.3

9. Appendix II – Anti-plane model - Script

```
clc
clear
close all

% INPUT

b1=8.7;                                 %insert radius
bp=17;                              %potting radius
P=10000/2;                          %insert design load
size=50;                            %linspace size
c=20;                               %core thickness
f1=1.2;                             %outer ply thickness
f2=1.2;                             %inner ply thickness
TAUcCRIT=760*0.00689476;            %core max shear stress,
input*conversione psi->MPa
% core SCXV 1/4 – 5052 – .0025 density 5.2
a=35;                               %insert proximity distance
Ef1=60000;                          %[GPa]elastic moduli of top face
sheet
Ef2=60000;                          %[GPa]elastic moduli of bottom
face sheet

%%%%%%%%%%%%%%%%%%%%%%%%%%%%%%%%%%%%%%%%%%%%%%%%%%%%%%%%%%%%%%%%%%
%%%%%%%%%%%%%%%%%%%%%
% CALCULATIONS

%%% 01 - TENSILE - OUT of PLANE LOADING [D.3]
r=linspace(bp,100,size);                    %cylindrical coordinate r
variable
d=f1/2+c+f2/2;                               %distance between the
face sheet middle
e=d/2;                                      %case of Ef1=Ef2 and f1=f2
Q=P./(2*pi*r);                              %transverse shear stress
[D.2-1]
D=(Ef1*f1*Ef2*f2*(d^2))/(Ef1*f1+Ef2*f2);
%sandwich plate stiffness [D.2-3]
%z = thickness coordinate measured from the 'neutral surface' of
the core
zf1=linspace(((d-e)-f1/2),(d-e)+(f1/2),size);      %f1 z variable
zf2=linspace(((-e)-f2/2),(-e)+(f2/2),size);       %f2 z variable
TAUc=Q./d;                                            %[D.2.4]
TAUf1=((((d-e)+(f1/2))-zf1)*(P/(2*pi*D*f1)))'*(1./r); %[D.2.4]
hyp. e=d/2 in case of Ef1=Ef2 and f1=f2, balanced laminate. so d-
e=0.5
TAUf2=((((e)+(f2/2))+zf2)*(P/(2*pi*D*f2)))'*(1./r); %[D.2.4] hyp.
e=d/2 in case of Ef1=Ef2 and f1=f2, balanced laminate. so d-e=0.5

Pcrit_Tensile=2*pi*bp*d*TAUcCRIT;                      %insert static
load carrying capability [D.3-2]
```

```
%%% 02 - COMPRESSIVE - OUT of PLANE LOADING

Pcrit_Compressive=(Pcrit_Tensile/2)+2*pi*bp*c*TAUcCRIT     %[D.6-
1]

SFsingleinsert=Pcrit_Compressive/P

%%% 03 - INSERT INTERACTION, 2 INSERTS LOADED IN THE SAME
DIRECTION

nIS1=1/2*(1+a/(5*bp*2))                %[19.1-3]
Pcrit_Compressive_INTERACTION=Pcrit_Compressive*nIS1
SF_2_insert=Pcrit_Compressive_INTERACTION/P

%%% 04 - INSERT INTERACTION, 2 INSERTS LOADED IN THE OPPOSITE
DIRECTION

Nic=0.9;                                %[19.2-1]

%%%%%%%%%%%%%%%%%%%%%%%%%%%%%%%%%%%%%%%%%%%%%%%%%%%%%%%%%%%%%%%%%%%
%%%%%%%%%%%%%%%%%%%%%

%COMPARISON ANALYTIC VS FEM RESULTS

%input dati fem iniziali

FEMr_off=[51.5996000000000;55.6367000000000;59.3879000000000;63.24
62000000000;67.2413000000000;73.6859000000000;80.9946000000000;91.
5721000000000;102.311000000000;114.209000000000;126.484000000000];
FEMr=FEMr_off-35;
FEMTAUc=[2.1;
1.77900000000000;1.54500000000000;1.34000000000000;1.1560000000000
0;0.947600000000000;0.810300000000000;0.632000000000000;0.50920000
0000000;0.413500000000000;0.339000000000000];
%Calcoli results

TAUconFEMr=P./(2*pi*FEMr)./d;
Delta=TAUconFEMr-FEMTAUc;
Percentage=Delta./TAUconFEMr;

%%%%%%%%%%%%%%%%%%%%%%%%%%%%%%%%%%%%%%%%%%%%%%%%%%%%%%%%%%%%%%%%%%%
%%%%%%%%%%%%%%%%%%%%%

%PLOT single insert loading

figure
plot(r,Q,'LineWidth',3);
title('Transverse shear stress')
xlabel('radial distance[mm]')
ylabel('Q [N/mm]')

figure
```

```
plot(r,TAUc,'LineWidth',3);
title('Core transverse shear stress')
xlabel('radial distance [mm]')
ylabel('TAUc [MPa]')

figure
P=plot(r,TAUc,FEMr,FEMTAUc,FEMr,Delta,'LineWidth',1);
title('Core transverse shear stress, Results Analytic vs FEM')
xlabel('radial distance [mm]')
ylabel('TAUc [MPa]')
legend('Analytical','FEM','Delta')



figure
contourf(r,zf1,TAUf1)
title('Upper ply TauZx')
xlabel('radial distance [mm]')
ylabel('zf1[mm]')
zlabel('Shear')
c = colorbar;
c.Label.String = 'f1 TauZX [MPa]';

figure
contourf(r,zf2,TAUf2)
title('Lower ply TauZx')
xlabel('radial distance [mm]')
ylabel('zf2[mm]')
zlabel('Shear')
c = colorbar;
c.Label.String = 'f2 TauZX [MPa]';
```